IPA Fifth Convention, Jakarta, June 7 - 8, 1976

RECENT DEVELOPMENTS IN LOGGING TECHNIQUES AND INTERPRETATION IN INDONESIA

BY

Yves M. PIRARD and William J. PRINS
Schlumberger Overseas, S.A.
Carlos CRAMEZ
Total Indonesie

ABSTRACT

The 70's have seen carbonate reservoirs become important in Indonesia. New logging and interpretation techniques have conjointly been developed.

The Dual-Laterolog (DLL)* simultaneously records a deep and a shallow laterolog and a Micro-Spherically Focused Log (MICROSFL)* which measures the resistivity of the flushed zone. This combination allows good determination of the true formation resistivity hence water saturation in cases where the Induction log reaches its limitations.

The Dual-Spacing Compensated Neutron Log (CNL) * combined with the Compensated Density Log (FDC) * allows easy differentiation between oil and gas in relatively clean reservoirs. Shaliness sometime render the interpretation less straightforward and deep invasion combined with high gas movability can make it very difficult indeed.

In carbonate reservoirs, the detection of dolomitized zones is important because of their usually higher porosity and permeability. The FDC-CNL is useful in that respect and CORIBAND * computation gives the percentage of dolomite after corrections for hydrocarbons and clay content. Also, CORIBAND allows identification of the transition zone and prevent costly mistakes in perforating zones with initial water-cut.

The 4-arm High Resolution Dipmeter (HDT) * has progressively replaced the 3-arm dipmeter. Its excellent resolution when combined with adequate software extends the field of dipmeter applications, one of which is the study of environment at the time of deposition in terms of prevailing energy. This in turn is used as a help to well-to-well correlation.

* Trade mark of Schlumberger.

INTRODUCTION

A Well Evaluation Conference was presented in Jakarta 1970. It contained a comprehensive review of the various logs run in Indonesia at that time and of different interpretation methods used in typical Indonesian sands and shales sequences. It was reviewed and re-edited in a more condensed form at the SPWLA 14th symposium in 1973 without major changes (17).

Meanwhile, new and more sophisticated logging tools were introduced, mainly the Dual Laterolog * - Rxo tool, the Dual - Spacing Compensated Neutron * and the High Resolution Dipmeter * New problems had also to be solved, related to the growing importance of carbonate reservoirs in the search for oil in Indonesia. This paper is meant to show examples of how the new tools can solve the new problems while giving better answers to the old problems.

APPLICATION OF THE DUAL LATEROLOG-MICROSPHERICALLY FOCUSED RXO LOG FOR BOTH DETECTION AND QUANTITATIVE EVALUATION OF HYDROCARBONS

Short list of Symbols used in the following text (for a complete list of Symbols see Reference 2 pages 1 and 2).

R_t	True (uncontaminated, non invaded zone) resistivity.	S_w	Water saturation (non invaded - zone).
C_t	True conductivity.	S_o	Oil saturation.
R_m	Mud resistivity.	S_{xo}	Filtrate saturation (flushed zone).
R_{xo}	Flushed zone resistivity		
R_w	Formation water resistivity		

Many years ago when the Electrical Log (ES) was the only resistivity device, the need was felt for a deep reading R_t tool when the ratio R_t/R_m was high (either due to high R_t , or low R_m or both) and the ES no longer accurate, e.g. in carbonates or evaporites drilled with salty mud.

This gave rise to the design of a family of Laterologs , devices capable of sending a thin focused disc of current into the formation perpendicular to the borehole even at high R_t/R_m ratios and thus able to measure the formation resistivities under these conditions with the added advantage of good vertical definition.

The earlier tools of this type with wide field use were the Laterolog-7* (LL7) and the Laterolog - 3* (LL3). The "7" and "3" respectively indicating seven and three electrodes in the focusing system. The first tool, LL7 is also referred to as a "resistivity-measuring" and the LL3 as a "conductivity-measuring" device.

In the LL7 the measure current (i_o) is held constant, the tool detects the variation in voltage (V_o) which is proportional to the resistivity of the formation. The best accuracy is in high resistivities. To satisfy the need for improved accuracy at lower resistivities, the LL3 was designed : it maintains the voltage(V_o) of its three electrodes constant, the current (i_o) which varies with the formation conductivity is measured. Best accuracy is in the relatively more conductive formation, although the tool is also capable of being accurate at resistivities well over 1000 ohm-m.

A further need arose to increase the working range of the tools, at both very low and very high resistivities. To achieve this, both voltage and current are varied and measured but the product $i_o \times V_o$ is held constant.("Constant Power"). The first of these tools was the LL9 or "Sequential Dual Laterolog" (Ref. 4, 5). A further development, very similar to the LL9, is the Dual Laterolog-MICROSFL*. The range of resistivities it is capable of measuring, is from 0.2 to 40.000 ohm-meters. It provides the simultaneous recording of not only the deepest ever laterolog(LLd) but also of a "Shallow Laterolog"(LLs) and a third, very shallow (about 4" depth of investigation) device, the Micro-Spherically-Focused log (MICROSFL). The MICROSFL can be in short described as having in the desired shallow investigation depth of a Microlaterolog (MLL) and yet has the capability of ignoring the mud cake and rugose hole effects of the Proximity Log * (which tends to read too deep for an accurate R_{xo} measurement). LLd and LLs are mounted on a sonde (9 electrodes). The MICROSFL is pad mounted on one of the arms of a four arm centering linkage, which also provides a Caliper measurement. A Gamma Ray and SP (Spontaneous Potential) can be recorded simultaneously. The array of three investigation depths are well distribiuted allowing a determination of invasion diameter (d_i) and hence the possiblity of correcting R_{LLd} for d_i , resulting in an "R_t" . This is done with the help of Figure 1. (See also Ref. 2, Chart R_{int} - 9 , page 64).

Long established and still persistent in many minds is the idea that a Laterolog is a tool for very high resistivities only. The following will demonstrate that this is not the case, thus enhancing the usefulness of modern Laterologs.

What we are looking for here is quantitative hydrocarbon evaluation, not so much the detection of hydrocarbon bearing formations. It is interesting to compare the main deep resistivity devices here. Very broadly seen, as a detection device the Induction Log (6FF40) * starts to become preferred when $R_{mf}/R_w > 2$, while the Dual LL is better when $R_{mf}/R_w < 2$. (See Ref. 4). The latter has the advantages of 1) giving an immediate "Overlay" picture with the MICROSFL (R_{xo}) while if using the IES an extra run with an R_{xo} tool, plus tracing, is required and 2) vertical definition is much better with the DLL-R_{xo} (24 " current / measure sheet against 6' for the IES).

DUAL LATEROLOG – R_{xo}

LLd – LLs – R_{xo}

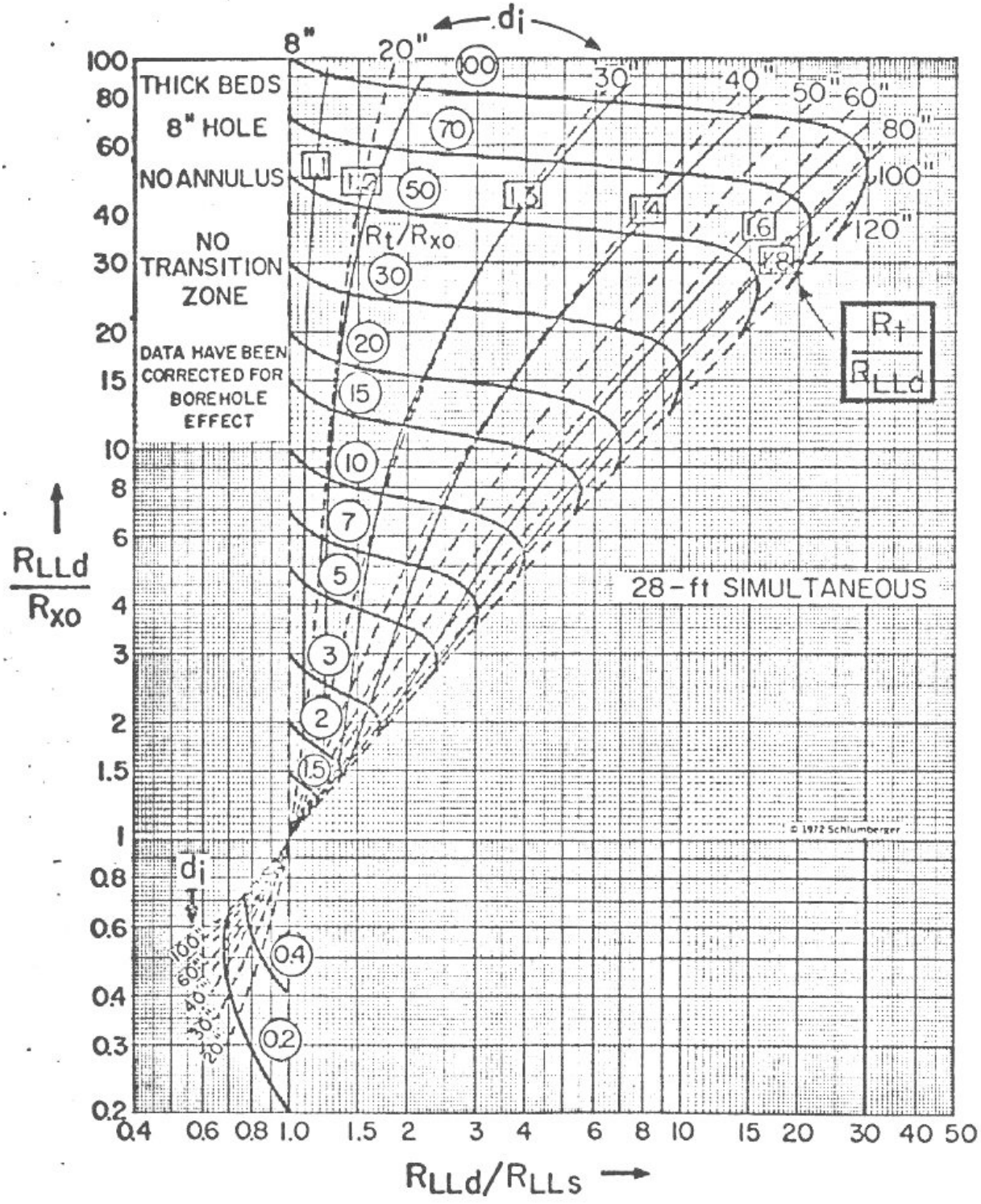

FIGURE 1 :

R_t and d_i determination with Dual LL - MICROSFL (Chart R_{int} - 9 page 64 Reference 2).

If an annulus is present during logging, the Induction capability loses some ground.

It is to be noted that the ratio R_{mf}/R_w is not the only criterion to be applied. More important is the ratio R_{xo}/R_t, as well as the absolute value of R_t itself. The latter limits Induction usage to 100 ohm-m maximum.

Generally we can say that for invasion diameters of more than 30" and $R_t/R_{xo} > 2$ the LLd gives a better R_t than the 6FF40.

In Indonesia R_t/R_{xo} is nearly always > 2 in hydrocarbon bearing formations. For $R_t/R_{xo} = 2$ and $S_w = S_{xo}^5$ we can use the plot of Figure 2. (See also Ref. 4). A step profile of invasion is assumed and the R_{mf}/R_w ratio is plotted against S_w. The dashed line defines the border line between the two regions where either 6FF40 Induction or Laterolog should be preferred. Here we see that a better R_t is obtained by the LL if $S_w \leq 40\%$ and $R_{mf}/R_w \leq 2.5$. Both conditions are prevalent in most Indonesian hydrocarbon bearing reservoirs. If S_w cutoff is set at 30% the R_{mf} / R_w range goes to 3.5 and for $S_w = 20\%$, R_{mf} / R_w is as high as 7.

If a strong annulus is present, a condition which exists often at the time of logging, the Laterolog area is much increased : see the solid curve on Figure 2. In this case all Indonesian reservoirs are well within the Laterolog area.

Following are a few examples of Dual Laterolog-MICROSFL, as well as some Induction logs, in Indonesian reservoirs.

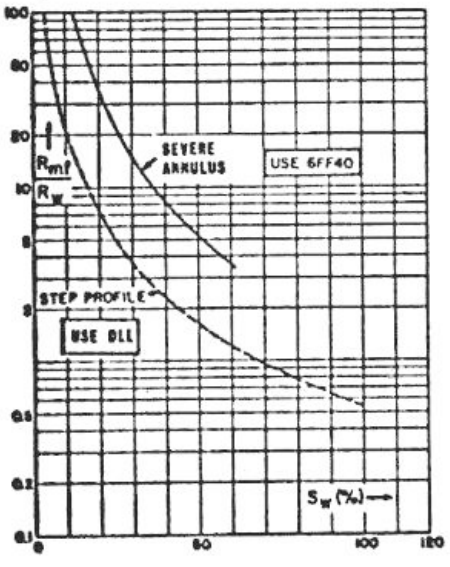

FIGURE 2 :

Best tool for R_t determination. $\frac{R_t}{R_{xo}} \approx 2$. Based on $\frac{R_{mf}}{R_w}$ and S_w, for step profile (dashed curve) and severe annulus (Solid curve).

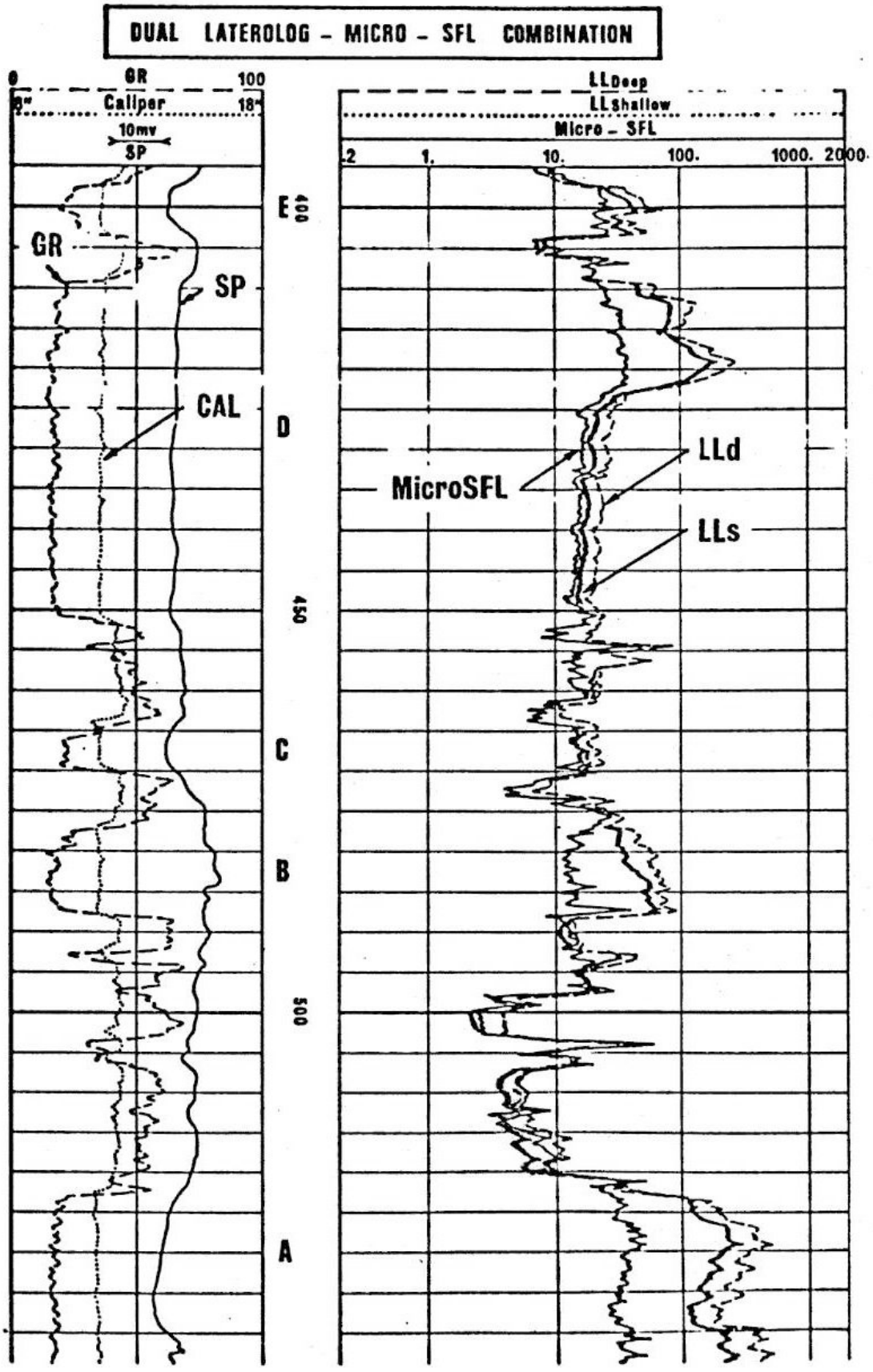

FIGURE 3 : Example 1 Dual Laterolog-MicroSFL combination for Quick Look.

The first example (Figure 3) shows a sand shale series where it is clear at a glance that there are at least four zones of interest.

Zone A, shows some separation between LLd and LLs and a large separation between LLs and MSFL, indicating invasion and most certainly hydrocarbons. The Gamma Ray shows the sand as quite clean, with a slightly negative SP.

Zone B is similar except for the fact that the SP is slightly positive here. This may well indicate (fresher) water rather than hydrocarbons. (This was confirmed by detailed calculations and subsequent Drill Stem Tests).

Zone C shows a deeper invasion and a higher Gamma Ray indicating some higher clay content. Resistivity is lower than in A and B, however one might still conclude that there may be some hydrocarbon, but examination of the lower part of zone D condemns zone C as most probably water bearing.

Zone D looks clean, quite homogeneous with again a slightly negative SP indicating R_w again lower then in zone B, and has a clear hydrocarbon water contact (at 422 m).

Zone E is a continuation of D, but is somewhat more shaly which causes resistivity to be lower.

Thus this log gives an immediate look at the section, all in one single log run It gives clues as to hydrocarbon content, sand thickness, shaliness as well as to permeability and movability, as will be seen in some more detail in the following examples.

In addition this log provides an easy guide for the Wellsite Geologist or Petroleum Engineer for further action, such as the decision of where to shoot sidewall cores, where to run Formation Interval Tests or plan Drill Stem Tests.

COMPARISON LATEROLOG – INDUCTION IN HIGH RESISTIVITY FORMATIONS

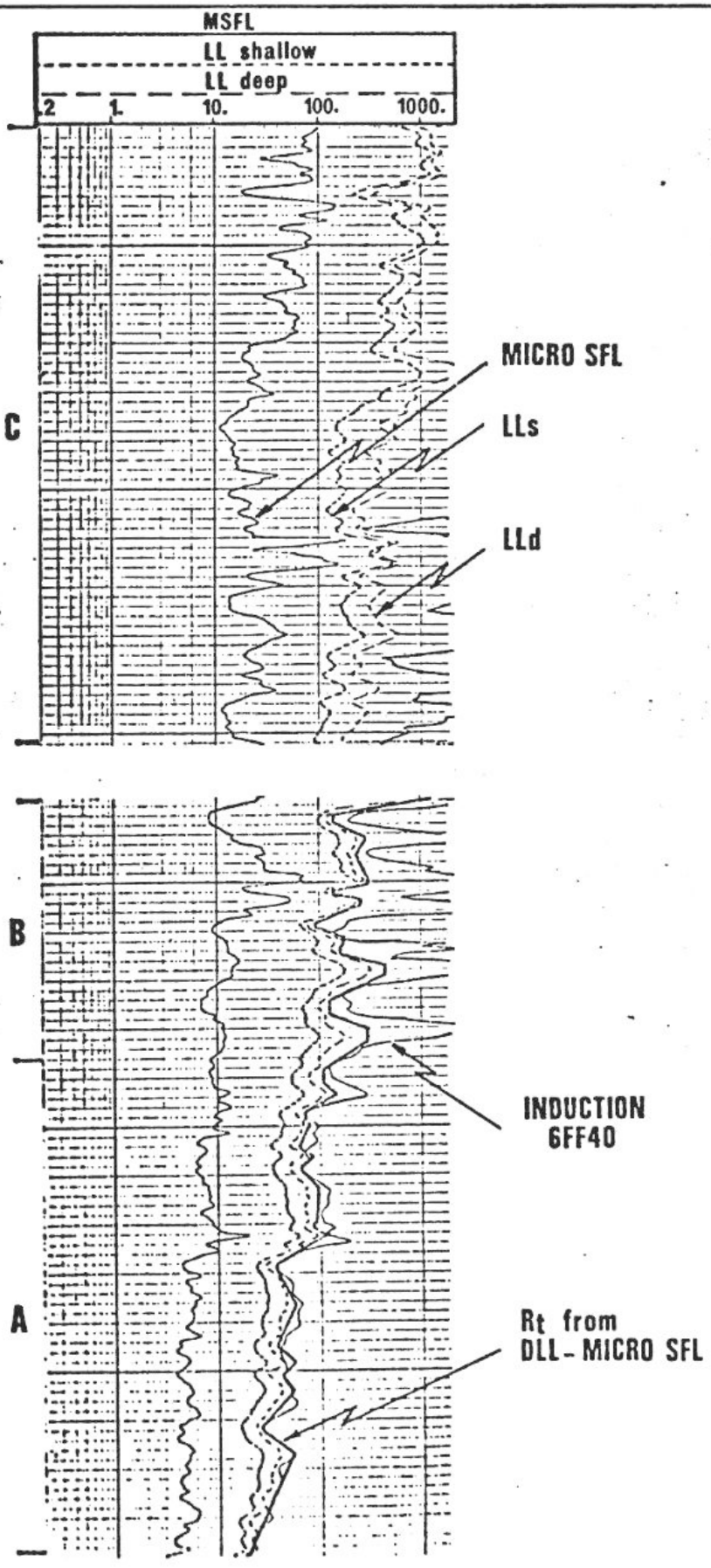

FIGURE 4 :

Example 2

Carbonate in Indonesia.

The second example (Figure 4) is of a Dual Laterolog-MICROSFL log and 6FF40 Induction Log in an Indonesian carbonate section. Also shown on Figure 4 is an R_t derived from the Dual LL-MICROSFL with chart R_{int} - 9 (of Ref. 2 page 64).

At first glance we see a steadily increasing resistivity through zones A and B and a more constant value through zone C. This is indicative of a long transition zone through A and B. Zone C may well be at irreducible water saturation (Ref. 9).

The Induction Log alone would rather suggest an Oil Water Contact at the border of zones A and B with a shorter transition zone below. Part of zone B and practically all of C shows the Induction Log incapable of coping with the high resistivities, even in this $8\frac{1}{2}$" hole and not very salty mud.
The borehole signal is in this case always small and negative (around 2 mmhos/m) : This means that at a true resistivity of 100 ohm-m (conductivity C_t = 10 mmho/m) the 6FF40 tool reads C_{IL} = 10-2 = 8 mmho/m or 125 ohm-m
at R_t = 200 (C_t = 5) , C_{IL} = 5 - 2 = 3 mmho/m or 333 ohm-m
at R_t = 400 (C_t = 2.5) , C_{IL} = 2.5 - 2 = 0.5 mmho/m or 2000 ohm-m
(meaning the curve now reaches the edge of the film scale).
at R_t = 400 (C_t = 2) , C_{IL} = 2 - 2 = 0 mmho/m or ∞ ohm-m,
hence the sharp excursions of the 6FF40 curve to the right and well off scale.

Added to this (Ref. 1, 2, 4) is the effect of the zero drift $\pm$ 2 mmho/m that each tool has, as well as the possible change in "Standoff" due to the sonde being at times centered in the hole, change of hole size and consequent changes in borehole signal. We may therefore conclude that in zone C, the "pay zone", the DLL-MICROSFL is a must. Looking at zones A and B we see that R_{IL} and R_t (from DLL-MICROSFL) are in fair to good agreement.

In conclusion : for hydrocarbon detection alone either 6FF40 or DLL may do, but for reliable evaluation of resistivity and consequently of hydrocarbon saturations, the DLL-MICROSFL is a must in the pay zone and in addition, it gives a much better definition of the transition zone (See also Ref. 9, Example 1).

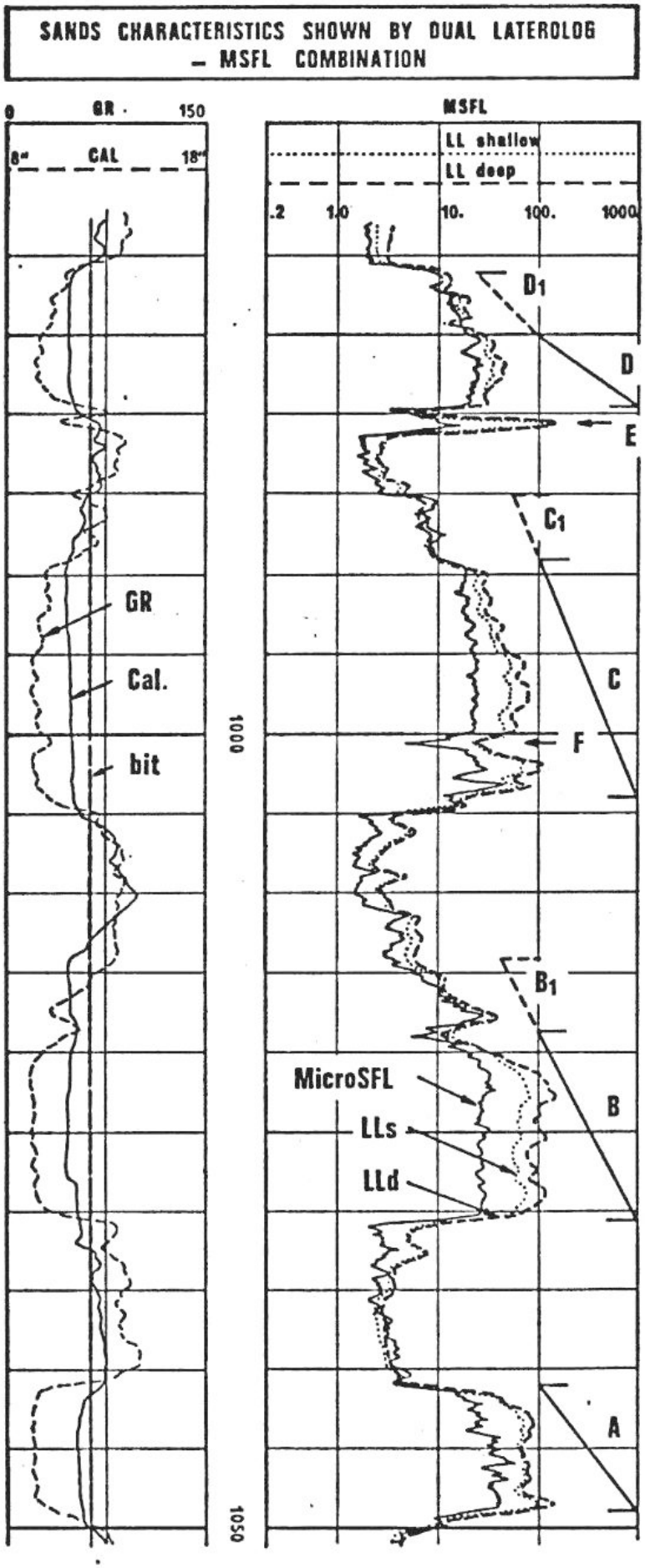

FIGURE 5 : Example 3

Sand-shale sequence in Indonesia. Indication of sand characteristics.

Figure 5 shows another example of a Dual LL-MICROSFL/GR/Caliper, this time in a sand shale sequence, giving an immediate idea of the section as far as hydrocarbon presence is concerned as well as good indication of sand quality, permeability and hydrocarbon movability.

Good vertical resolution shows sharp bed boundaries as well as vertically thin features such as the lignite bed at 980.5 m (E on Figure 5) and the thin shale break at 1000.5 m (F on Figure 5).

The separation between the three resistivity curves gives an indication of some relative sand characteristics :

Sand A : very small separation between LLd and LLs, large between LLd and MICROSFL. This indicates shallow invasion and consequently good porosity and permeability. The large separation between LLd / LLs and MICROSFL is an indication of moved hydrocarbons. In short : a good reservoir. (Chart R_{int} - 9 Ref. 2 page 64 gives a d_i around 20").

Sand B : similar in resistivity range, but larger separation between LLd and LLs, indicating deeper invasion (Chart gives a d_i of 30-35 inches), probably due to lower porosity. Still a good reservoir, but probably a finer grained sandstone.

Sand C : looks not dissimilar to B but has, starting at 995 m towards the top, increasingly lower resistivities with similar invasion depths as sand B (confirmed by plotting on the chart to be around 35 inches). The lower resistivities are probably due to increased clay content, which is confirmed by the Gamma Ray.

Sand D : has lower resistivities, less separation between LLd and LLs, indicating less deep invasion (Chart : d_i = 20 - 25 inches). The lowermost 4 - 5 meters look still fairly good. Then increasingly, the three curves start to lose separation. (zone D_1 on Fig. 5). This indicates lack of invasion due to low permeability. The same reduction in separation between the three curves can be seen in zones B_1 and C_1. Here, the Gamma Ray also shows large increases, indicating increased clay content. In D_1 however, the Gamma Ray deflections remain much lower, this means that the reduction of permeability in this sand is due to decreasing grain size, in other words increasing silt, rather than clay content.

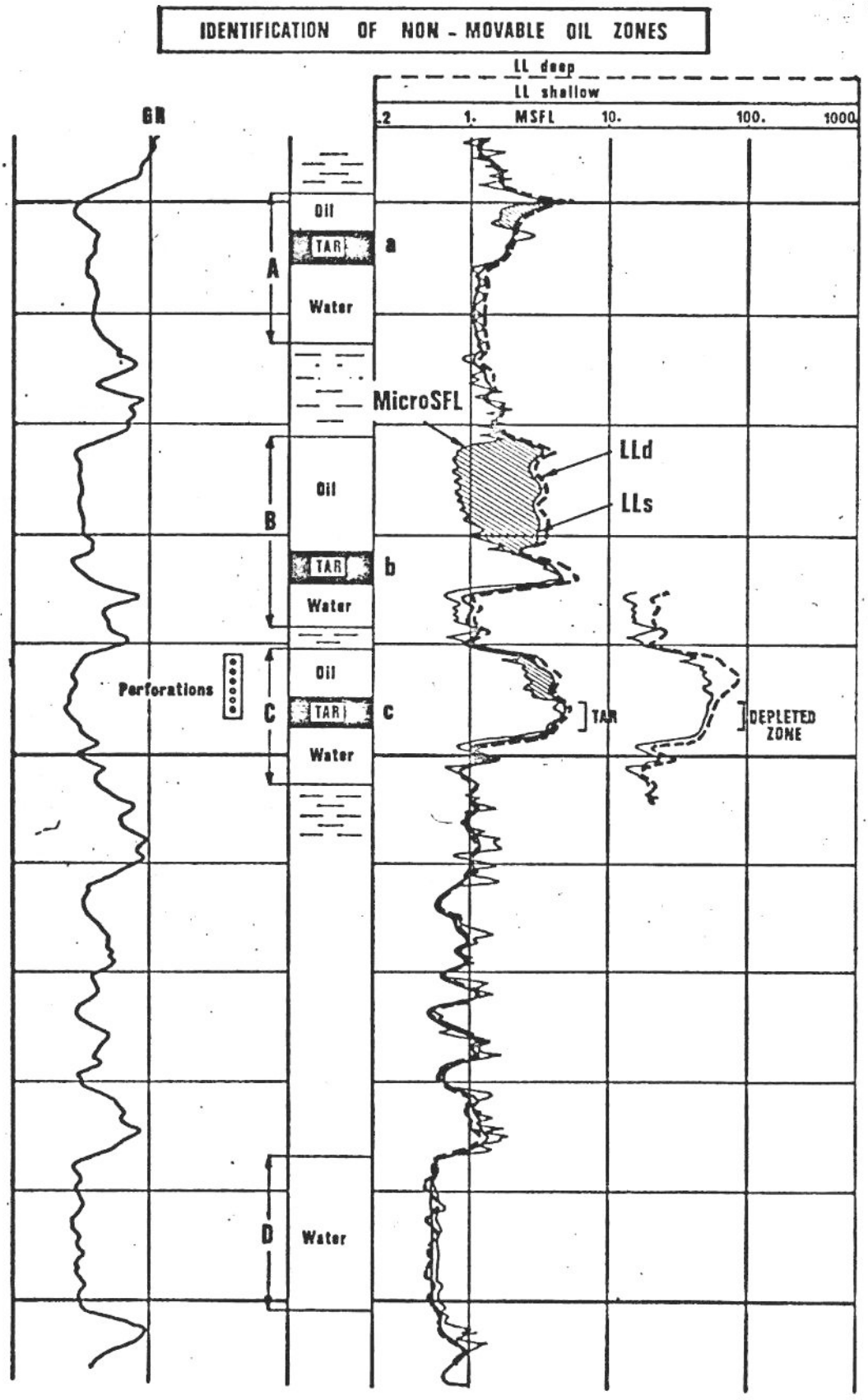

FIGURE 6 : Example 4

Identification of non-movable hydrocarbons.

Figure 6 shows again a sand/shaly sand/shale sequence. R_{mf} and R_w are about equal, which is confirmed by SP (not shown) and sand D, which is undoubtedly water bearing with a resistivity of 0.6 ohm-m. (LLd ≈ LLs ≈ MSFL). All three sands A, B and C higher up in the well show hydrocarbon - water contacts with LLd ≈ MSFL in the water and LLd ≫ MSFL in the hydrocarbon (in this case oil) bearing parts.

In each of the sands however, the oil bearing part shows distinct section where LLd = LLs = MICROSFL (indicated with a, b and c on Fig. 6). The high resistivity indicates oil, but the fact that $R_t \approx R_{xo}$ (or $S_w \approx S_{xo}$) indicates that this oil is not moved by the invasion process : zones a, b and c are tar mats or heavy, viscous oil not uncommonly found just above an oil-water contact.

The upper sections of A, B and C sands (cross hatched on Fig. 6) show fair to good movability of the oil.

Zone C, perforated across oil and tar, produced 1250 barrels of clean oil per day.

It is important to note that a depleted zone would also show S_w to be equal to S_{xo} (LLd ≈ MICROSFL in this case of $R_w \approx R_{mf}$). The resistivity of a depleted zone measured by a deep reading tool would be higher than that of the water zone, while being lower than the deep resistivity measurement in the not yet depleted zone. This condition is illustrated by the short log section shown on Figure 6 to the right of zone C.

In conclusion :

The Induction log has long been the main device in Indonesia used for detection of hydrocarbons as well as for reservoir evaluation, possibly leading to a pessimistic estimation of oil saturation.

If for hydrocarbon detection the Induction log remains an excellent device, the newer Dual Laterolog - MICROSFL has shown itself to be the better tool for quantitative evaluation in practically all reservoirs in Indonesia, both sandstones and carbonates. Water saturations from the DLL - MICROSFL are found to be considerably lower, often by a factor of 1.2 to 2.

As a hydrocarbon detection tool the DLL-MICROSFL offers valuable "Quick-Look" information such as sharp bed definition (2' for the DLL-MSFL compared to 6' for the Induction Log), invasion depth, movability of the hydrocarbons, permeability, sand quality.

A further important advantage is the reduction of valuable rig time.

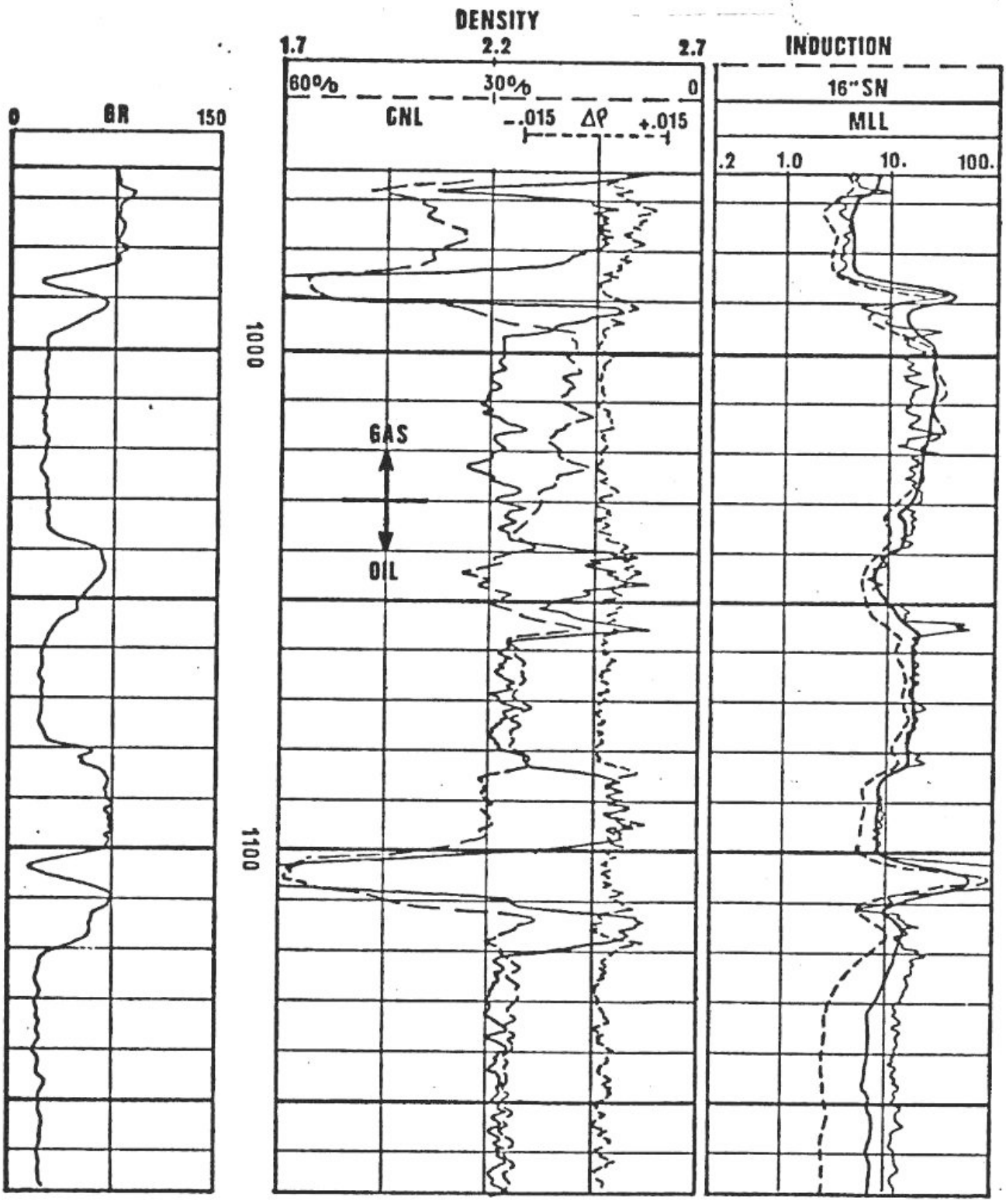

FIGURE 7 :

In this clean shales-sand series, the overlay Microlaterolog - Induction detects hydrocarbons in the two upper sands above 1080'. The FDC-CNL indicates a gas-oil contact at 1030'. Note also the good definition of the coal beds at 986' - 990' and 1100' - 1108' by the FDC-CNL.

APPLICATION OF THE COMBINATION COMPENSATED FORMATION DENSITY LOG (FDC) * DUAL-SPACING NEUTRON LOG (CNL) * TO GAS - OIL DIFFERENTIATION

The inverse effects of gas on the Formation Density log and a Neutron log have been used for years to differentiate between oil and gas in hydrocarbon bearing reservoirs and several examples have been shown in various papers. At the time of the presentation of the Well Evaluation Conference - Indonesia in 1970, the most sophisticated Neutron available was the Sidewall Epithermal Neutron (SNP)*. It was recorded separately from the Formation Density log, and this made it necessary to make an overlay of the two logs in order to identify gas bearing zones. In addition, the porosity measurement was adversely affected by bad hole conditions.

Early in the '70s, a new neutron device was introduced : the Dual - Spacing Neutron Log (CNL) (6) (7). Its main advantage is its combinability with the Compensated Formation Density Log (FDC) . The two curves are recorded simultaneously allowing for quick, easy identification of gas zones in relatively clean and simple lithologies. Figure 7 and 8 show two such examples. In both cases, the Induction Log (IES) is also shown, with the Microlaterolog (MLL) overlaid. This overlay identifies easily the hydrocarbon bearing zones in both cases.

Fig. 7 is an example of a clean sand/shale sequence. The IES-MLL overlay shows the lower sand, below 1120', to be water bearing and the upper sands, above 1080', to be hydrocarbons bearing. The separation between the Density and Neutron curves is what one would expect in sands up to 1030'. Above this depth, there is a marked change in separation with the Neutron reading suddenly appreciably less porosity than the density. This feature is characteristic of the presence of gas. Its effect is to decrease Neutron porosity and increase the apparent porosity from the Density (in fact, decrease the Density readings) resulting in a large separation between the two curves. We can safely conclude at a gas-oil contact at 1030'. Note also the sharp definition of the coal beds at 986 - 990' and 1100 - 1108'. Both Density and Nutron go off-scale towards high porosities, the Gamma-Ray reads minimum value and the resistivity curves, especially the MLL because of its good vertical resolution, shoot to high resistivities.

* Trade mark of Schlumberger.

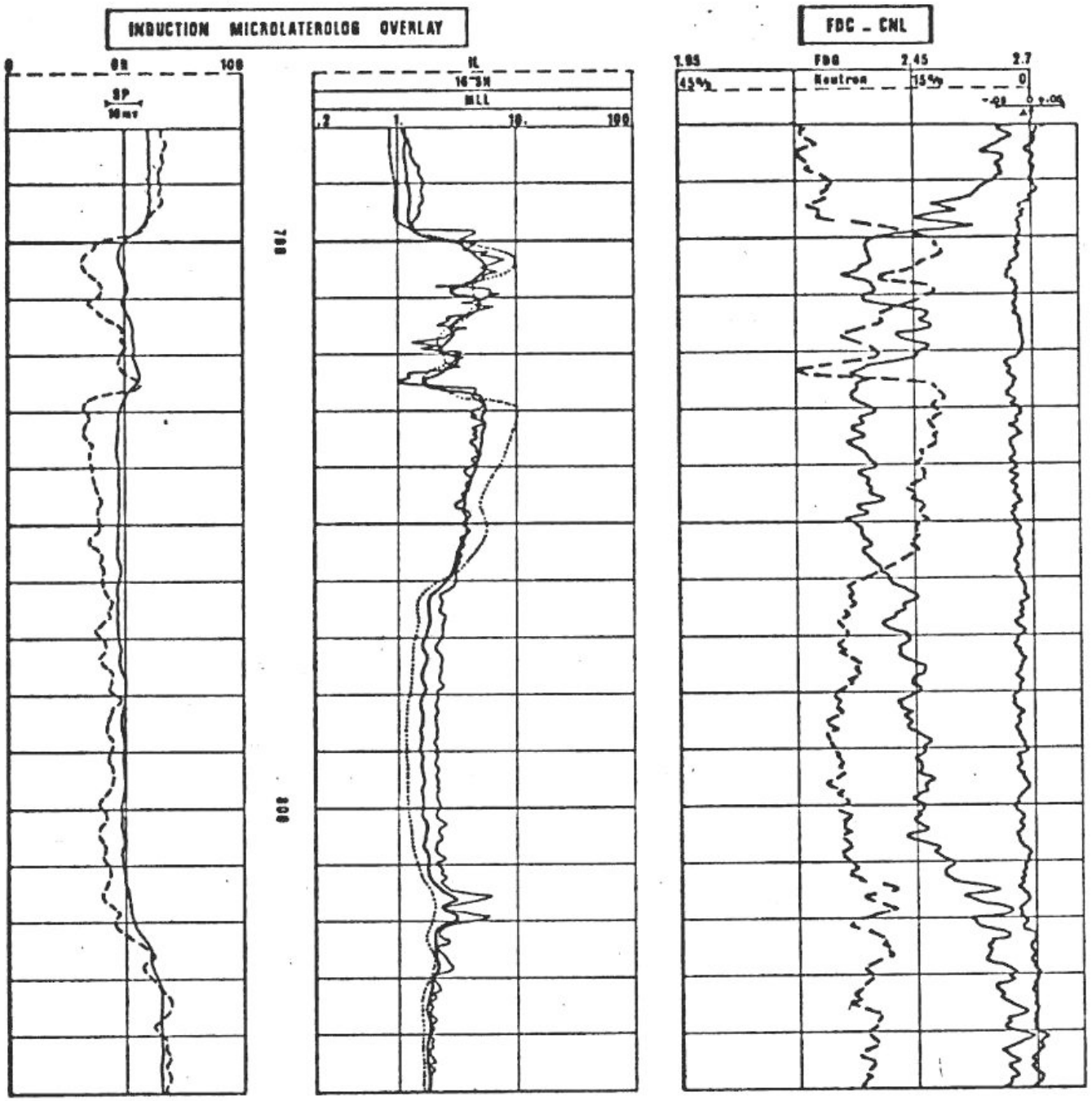

FIGURE 8 :

The overlay Induction-Microlaterolog clearly indicates an hydrocarbons - water contact at 760'. The hydrocarbon is easily identified as gas by the FDC-CNL log. Lithology is glauconitic sands which explains the large, shale-like, separation in the water-bearing zone.

In Fig. 8, the lithology is glauconitic sand hence the separation between the Neutron and Density curves below 760'. The presence of glauconite in the sand explains the relatively high radioactivity level throughout the sand (40 to 45 API compared to 10 - 20 API for a clean quartz sand). At 760', the IES-MLL overlay shows a hydrocarbon - water contact, and the FDC-CNL identifies the hydrocarbon as gas. Note the zone at 712' - 724' : the separation is again similar to what it was below 760'. This is due to shale content as confirmed by the GR and resistivity curves. The consistent negative density correction ($\Delta\rho$) is due to baryte in the mud (Mud weight : 13.6) resulting in heavy mud-cake.

As mentioned for the previous example, shales and clay have an opposite effect to that of gas on density and neutron measurements. This is due to their high bound water content. So it becomes difficult to identify gas zones if the formations are shaly and correction for shaliness must first be applied. In difficult cases, it becomes necessary to compute the density of the hydrocarbons in the formation (ρh) to make the differentiation. This necessitates the knowledge of the residual hydrocarbons saturation in the flushed zone (Srh = 1 - Sxo) and in turn requires to have a measurement of the resistivity in this zone (Rxo). It will be obtained from a micro-resistivity survey such as the Proximity log, the Microlaterolog or the MICROSFL which is recorded simultaneously with the Dual Laterolog. Knowledge of Srh is in any case necessary to correct porosity measurements for the hydrocarbon effect to arrive at the true porosity.

There is however a convenient way to take the shale effect into account without going to lengthy calculations. Under normal conditions, in a shale / sand sequence, the Gamma-Ray curve is a good indicator of shaliness. If one plots the difference in apparent porosities derived from the Density and Neutron measurement, which is an indication of shaliness, versus Gamma - Ray readings in the sands throughout the interval under study (provide the length of the interval is such that enough data can be gathered), a linear relationship can be established between (ϕD - ϕN) and GR for the oil and water bearing reservoirs. The presence of gas will cause the corresponding levels to plot outside of the trend thus defined because then the gas effect will counteract the shale effect thus changing (ϕD - ϕN) for a given level of radio-activity in the sand.

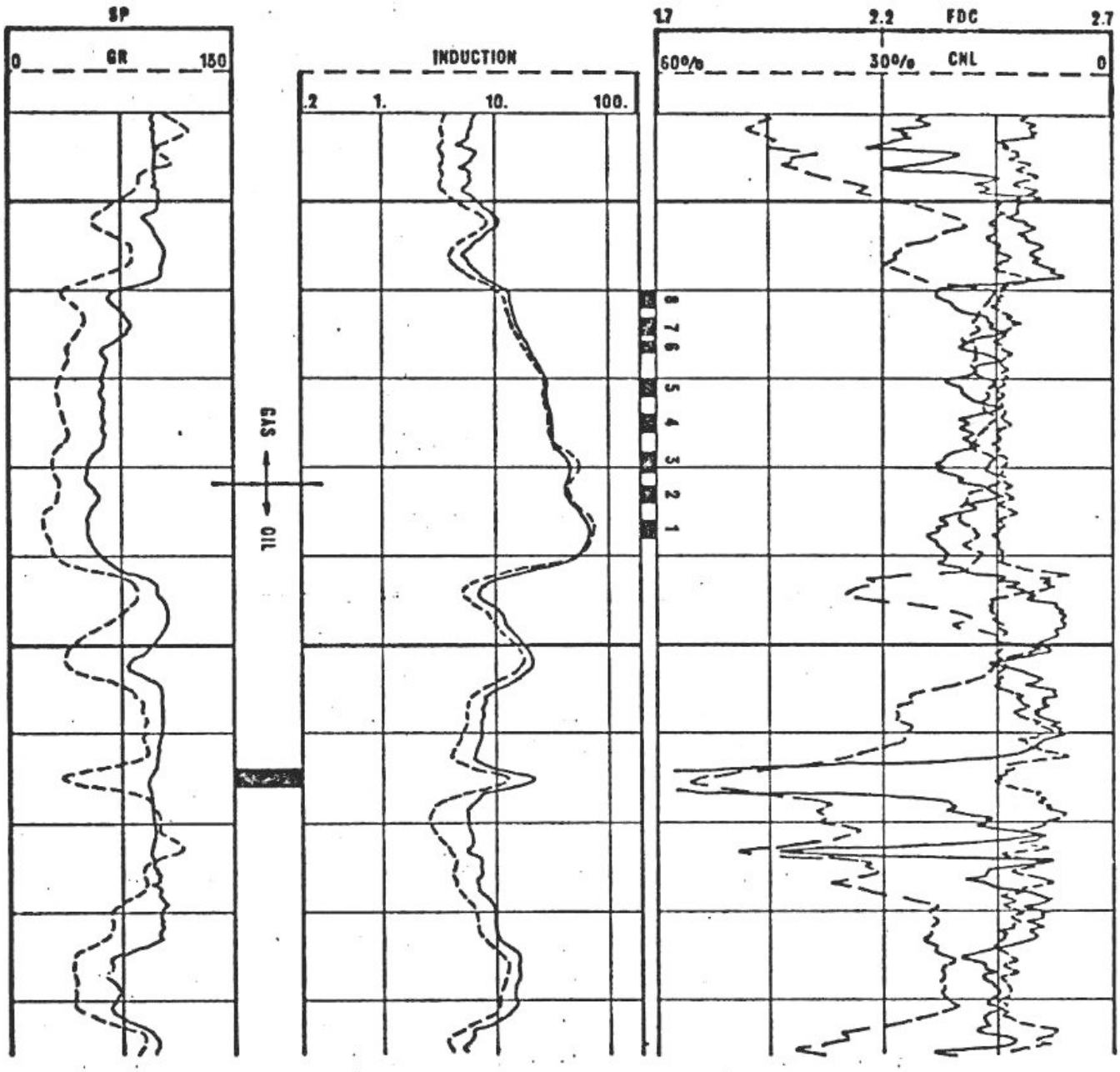

FIGURE 9 a :

Differentiation between oil and gas in this example is complicatedly the presence of clay in the sand as shown by GR, SP and a Resistivity curves.

Such an example is shown on Fig. 9 a. There is no obvious gas effect on the Density-Neutron combination in the sand at 1010 - 1042'. But when the levels shown throughout the sand are plotted on the GR vs (ϕD - ϕN) plot on which the oil-water zone has been established for the whole well (Fig. 9 b), it becomes obvious that levels 1 and 2, at the bottom of the sand, are oil bearing while levels 3 to 7 are gas bearing. The reservoir was originally thought to be entirely gas bearing from a test made by perforating the top part. But it was found later to be oil-bearing in nearby structurally deeper wells, confirming the gas-oil contact predictable from the logs at 1032' between levels 2 and 3.

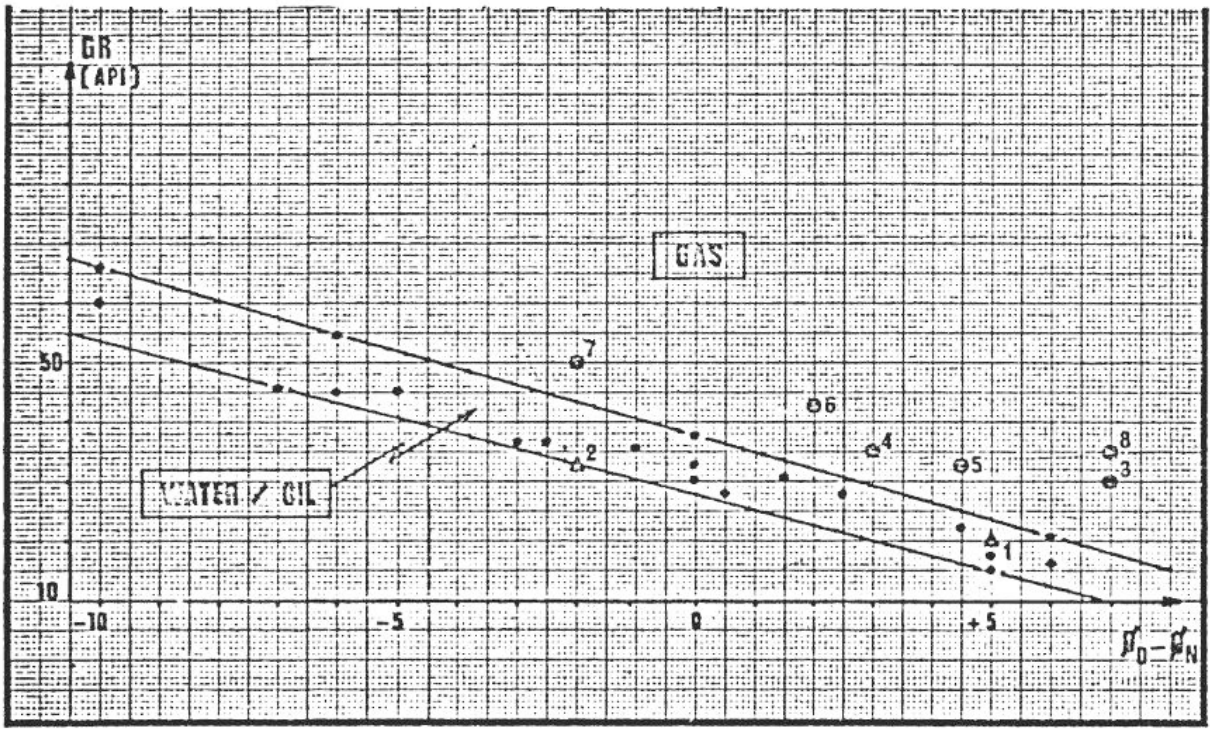

FIGURE 9 b :

This simple plot shows the gas-oil contact to be between levels 2 and 3

Another effect can render the interpretation difficult. To have a detectable effect on the logs, it is necessary that enough gas is present near the borehole. Most nuclear devices have shallow investigation, of the order of 8" to 10". So if the hydrocarbons have been thoroughly washed out by mud-filtrate invasion, interpretation will not indicate gas. The situation has improved with the introduction of the CNL which "sees" further away from the borehole than the SNP. But there are still some cases when combination of large invasion, high gas movability and small but noticeable amounts of shaliness render even sophisticated interpretation methods practically useless to differentiate between oil and gas.

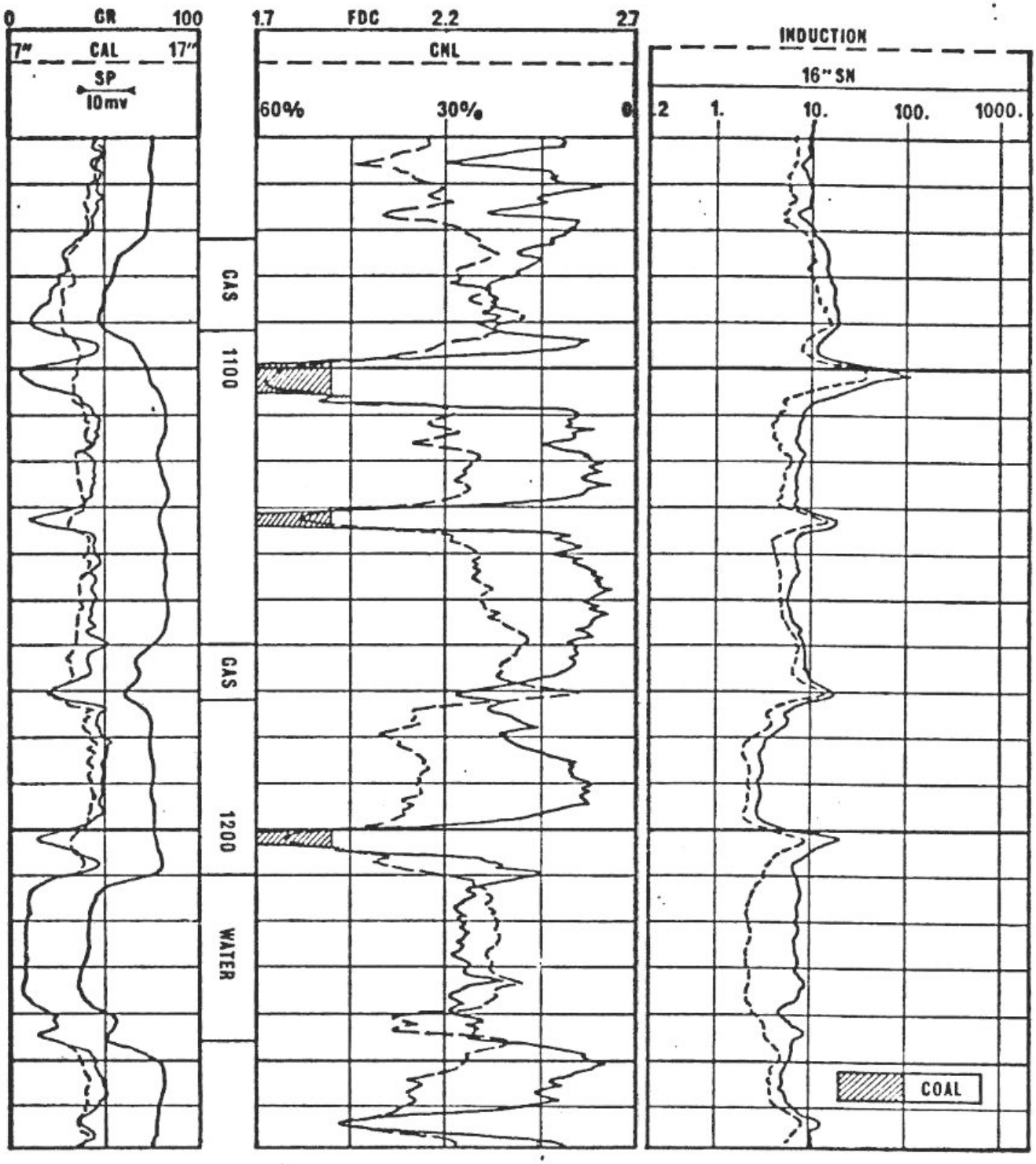

FIGURE 10 :

The sand at 1070' - 1095' is shown to be hydrocarbons bearing by the Induction log, The lack of tell-tale separation between FDC and CNL curves even in the cleanest part at the bottom leads to believe that the sand is oil bearing. In fact, it tested dry gas. This is explained by large invasion and high movability of the gas. The sand at 1160' - 1172' is clearly picked-up as gas bearing.

Fig. 10 shows a log recorded in the shaly sands sequence as in Fig. 7 in a nearby well. The sand at 1070 - 1095' is relatively clean at bottom but no tell-tale separation can be seen on the Density-Neutron. Complete calculations lead to ϕ_h = .65 to .7, and the conclusion was : oil. But it was perforated and produced dry gas.

A study of the water sands above and below concludes at an invasion of 120" or more. (This was arrived at by plotting the ratios R_{xo} / R_{ind} and R_{xo}/R_{SN} on the chart of Fig. 11). Also it shows that the percentage of residual hydrocarbons near the borehole within the investigation of the Proximity log (Not shown) which is quite comparable to that of the nuclear devices is in the range 5 to 10%. This is insufficient to result in any noticeable effect on even the CNL. The large invasion and low residual saturation are easily explained by the mud characteristics : weight was up to 16.5 and waterloss as high as 16. In the nearby well, where mud weight was 11.9 and waterloss 7, the same study shows only 30" of invasion in the same sands. There, differentiation between oil and gas was easy as demonstrated by Fig. 7.

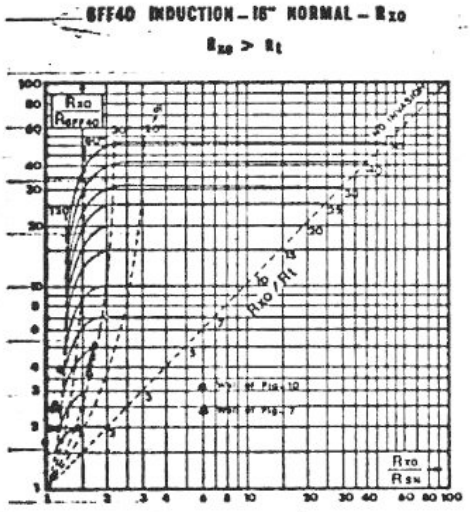

FIGURE 11 :

This plot clearly shows that the invasion in the well of Fig. 10 is much larger than in the well of Fig. 7.

In conclusion, we can say that differentiation between oil and gas is possible under normal circumstances and often easy from the Density-Neutron combination. Shaliness can be corrected for without too much trouble. But deep invasion and high differential pressure between mud column and formation might flush the gas so thoroughly that its identification becomes impossible.

The CNL makes it easier as it is recorded together, with the density, giving the log good visual appeal. It is borehole compensated so not affected by bad holes and it can in some instances "see" gas better than SNP because of its deeper investigation. In addition, its combinability with the FDC is an appreciable rig-time saving factor. A micro-resistivity measurement is useful for the differentiation in difficult cases and necessary to arrive at the true porosity in case of light hydrocarbons.

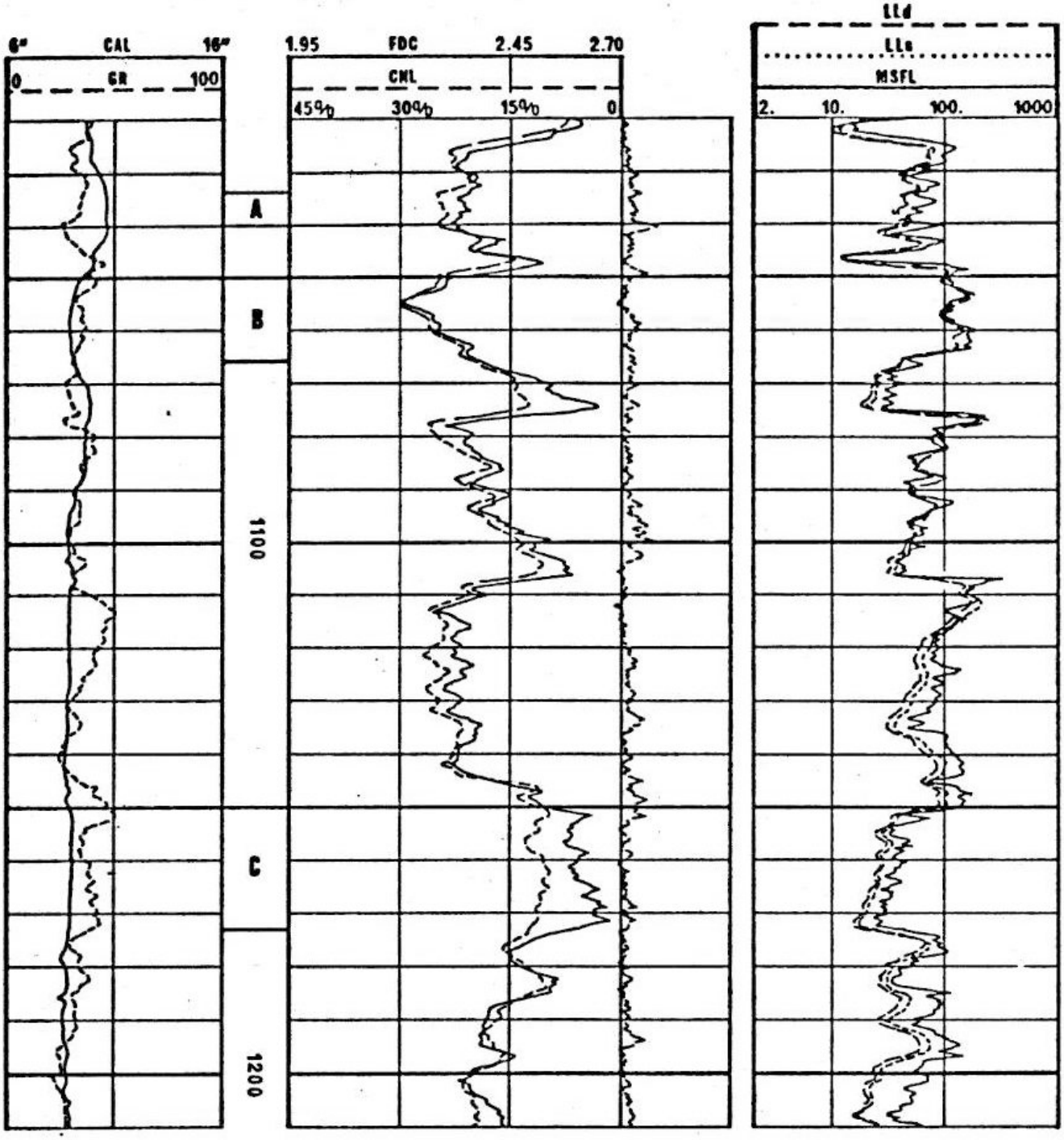

FIGURE 12 :

FDC and CNL have been recorded with limestone compatible scales. Zone B is identified as limestone by the absence of separation between the two curves, while zones A and C seem to contain an appreciable amount of dolomite.

APPLICATION OF COMPUTER PROCESSED INTERPRETATION TO CARBONATES PROBLEMS

The FDC-CNL combination has uses other than just differentiating between oil and gas. The responses of the two measurements are inverse also in front of dolomites, with the Dual-Spacing Neutron showing more porosity than the Compensated Formation Density. So, in carbonate reservoirs, it becomes possible to differentiate between limestone and dolomite. Dolomite content of such a reservoir is an important data and is often related to permeability if it comes from recrystallisation of the original limestone. It is often associated with secondary porosity.

If the FDC and the CNL have been run in limestone compatible scales, meaning that they will overlay in clean limestone, the CNL will read 16 limestone porosity units more than the FDC in front of a 100% dolomite formation. Any separation of the two curves within O and 16 p.u. will correspond to a percentage of dolomite such that :

$$\% \text{ dolomite} = \frac{\text{Separation}}{16 \text{ (p.u.)}}$$

An example is shown on Fig. 12. The FDC and CNL curves overlay perfectly over zone B defining it as pure limestone. Zone A shows 3 p.u. separation between FDC and CNL, indicating 18% dolomite. The separation between FDC and CNL varies from 8 p.u. at bottom to 5 p.u. at top of zone C, indicating from 50% to 30% dolomite.

In practice, the readings of the CNL and FDC have first to be corrected for clay content - in general small - and possibly hydrocarbons before the determination of the dolomite's percentage can be attempted. The clay content (Vcl.) is given by various clay indicator like GR, R_t, Neutron, cross-plots as explained in Ref. 8. Log readings are corrected for it then need to be corrected for hydrocarbons. The matrix density (ρma) is then derived (Fig. 13) and the percentage of dolomite can now be defined as :

$$\% \text{ dolomite} = \frac{\rho\text{ma} - 2.71}{2.87 - 2.71}$$

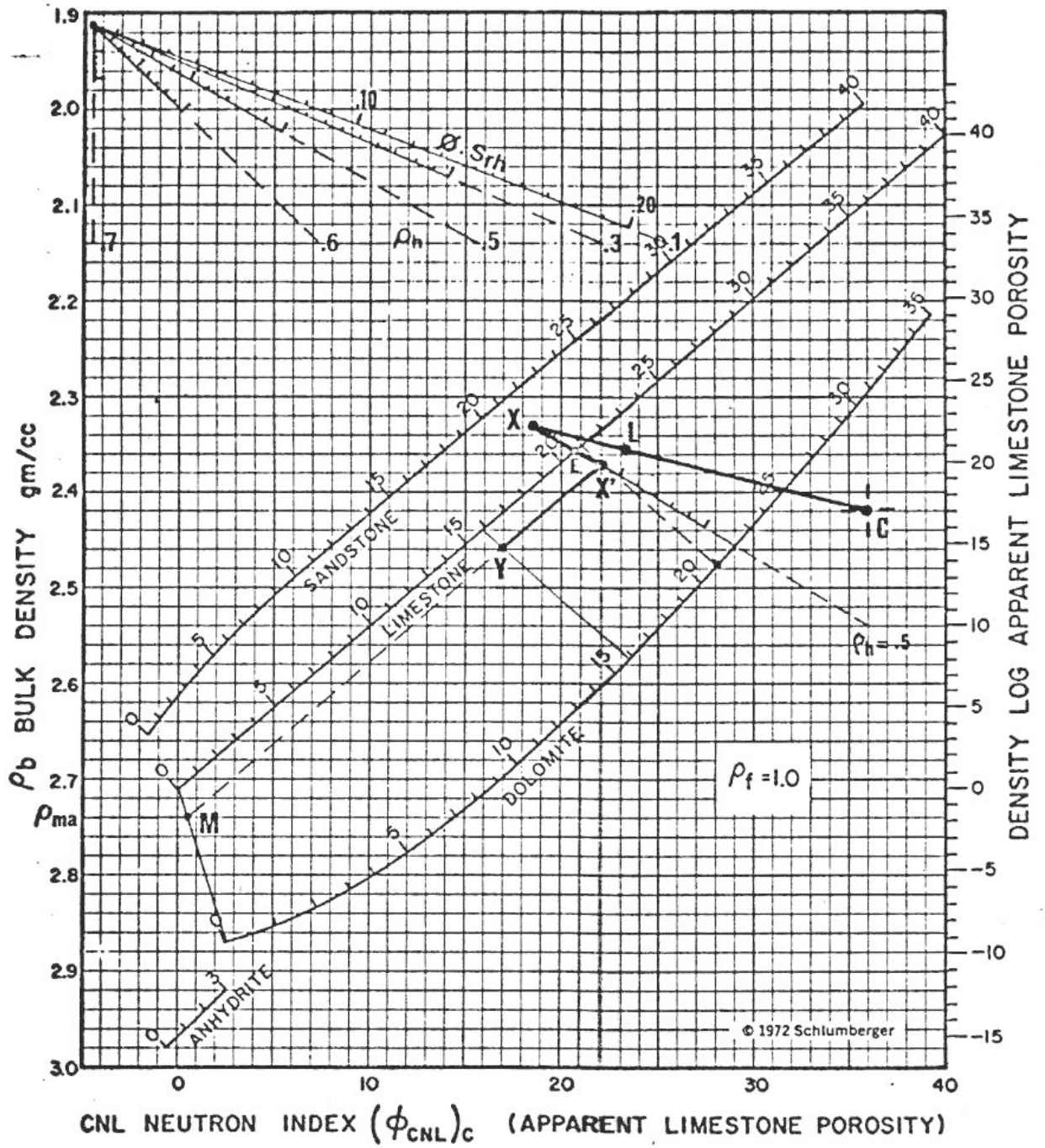

FIGURE 13 : Clay and hydrocarbons correction by CORIBAND

- C is the clay point, L is plotted from logs readings.
- X is such that XC = LC / (1 - Vcl.).
  It represents the clean part of the formation or (1 - Vcl.) % of the bulk.
- X' represents the clean part of the formation but the residuals hydrocarbons have now been replaced by water - ρma can be read at this stage.
- Y represents the formation after the clay has been replaced by matrix and the hydrocarbons by water. It has the effective porosity $\varphi = \varphi_{X'} (1 - Vcl.)$.

These calculations are lengthy and difficult to do continuously if one has to do them "manually". On the other hand, data can be fed to a computer which will process them quickly and and accurately. The CORIBAND program (Complex Reservoirs Interpretation By Analysis of Neutron and Density) is used. Its normal output in this respect is a matrix density curve scaled from 2.50 to 3.00. In this particular case, it is slighty modified to show a "% Dolomite" curve instead of ρma. It is best to record logs digitally on magnetic tapes which can be handled directly by the computer. Otherwise digitization of the optical logs, time consuming and error-prone, is necessary.

An example of CORIBAND is shown on Fig. 14. The heading is self - explanatory. On the first track are shown the % dolomite curve and a secondary porosity index obtained by difference between the total porosity and the the porosity derived from the sonic, taken to be equal to primary-intercrystalline / intergranular - porosity. In this example the most porous parts of the reservoirs seem to be associated with 10 to 25% dolomite and some secondary porosity.

If the % dolomite from the CORIBAND is compared to the one found by quick-look analysis of the FDC-CNL of Fig. 12 (Same well, same interval), some discrepancies are seen. CORIBAND shows 10 to 15% dolomite over interval B which looked like pure limestone on the log. This is due to the hydrocarbons correction. On the other hand, the top of zone C has only 20 to 25% dolomite against an apparent 30% from the logs. This is due to the clay correction : about 15% clay has been identified by CORIBAND. This percentage increases to 20% at the bottom of the interval. No dolomite is shown anymore because of a cutoff : above 15% clay, the % dolomite curve drops back to zero. Here, the clay indicator retained by CORIBAND was Rt. The GR is rather useless in this type of reservoir, and the cross-plots are affected by lithology.

On the second track one finds the water saturation of the reservoir and two curves giving the residual hydrocarbons volume and weight. The two curves would overlay each other if the hydrocarbons density was 1.00. As it is, the separation between the two is an indication of hydrocarbons density, in this case oil. This density is obtained before CORIBAND is attempted by pre-interpretation using the DET * program (Automatic Parameters Determination) or is input by the log analyst.

* Trade mark of Schlumberger.

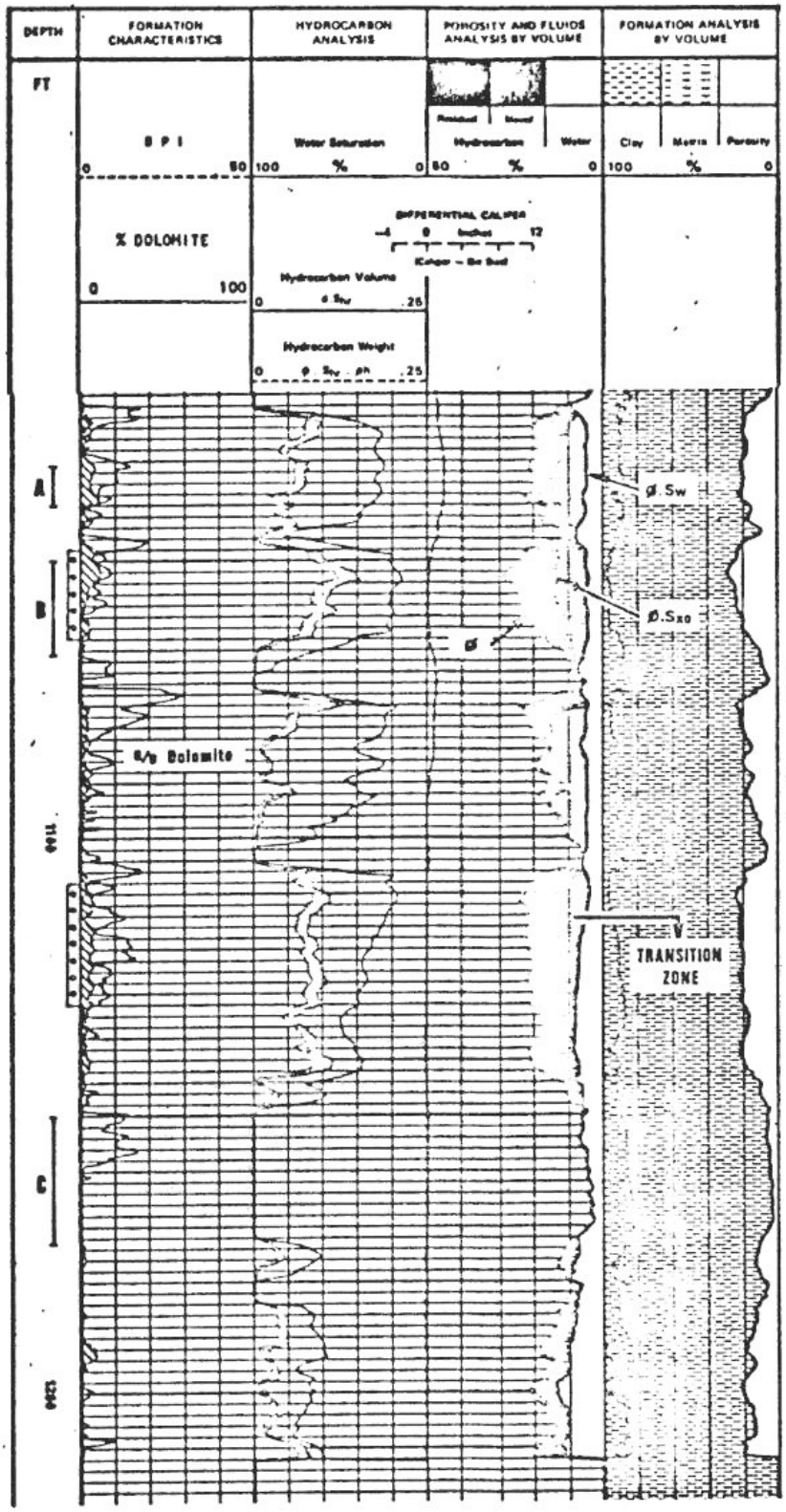

FIGURE 14 :

φ . Sw is constant down to around 1112', then starts increasing. The lower part of the log is thus interpretated as a transition zone. Zone 1108 - 1130' was perforated and produced 70 to 90% water, while zone 1048' - 1064' produced 1200 BOPD, no water.

An analysis of the fluids in the reservoir is given on the third track. Porosity is split between water ($\phi . S_w$) and hydrocarbons. In turn, these are split in moved and residuals hydrocarbons. The reservoir itself is analysed in track 4 which shows clay (Vcl.), matrix and fluid (ϕ) percentage.

An important application of CORIBAND was described in ref. 9. It is related to the concept of irreducible water, bound to the formation and immovable. The amount of irreducible water has been proved to be constant in a relatively homogeneous reservoir. If a reservoir contains more water than the irreducible amount, water-cut can be predicted. If it is at irreducible saturation, the production is water-free unless external water flows in through coning, high permeability zones (fractures) communicating with the water table or communication between zones behind casing because of poor cementation.

It is assumed that if $\phi . Sw$ is constant over a reservoir, it is in fact $(\phi . S_w)_{irr}$. If it starts increasing, or varies following the porosity, water-cut must be expected. $\phi . Sw$ is traced on the third track of the plot as mentioned above.

In this example, $\phi . Sw$ is quite constant down to 1112' then starts increasing indicating the start of a transition zone. The well was perforated at 1108' - 1130' and produced 70 to 90% of black sulphurous water. It was then plugged back and reperforated at 1048 - 1064' producing 1200 bopd., no water.

In addition to solving continuous lithology determination problems and allowing selective perforating to avoid interstitial water-cut, CORIBAND provides accurate values of porosity and water saturation hence is a great help for the determination of the reserves. Integration of both porosity and hydrocarbons in-situ is made and listed. And an indication of hydrocarbons movability is given by the difference between the two curves $\phi . Sw$ and $\phi . Sxo$.

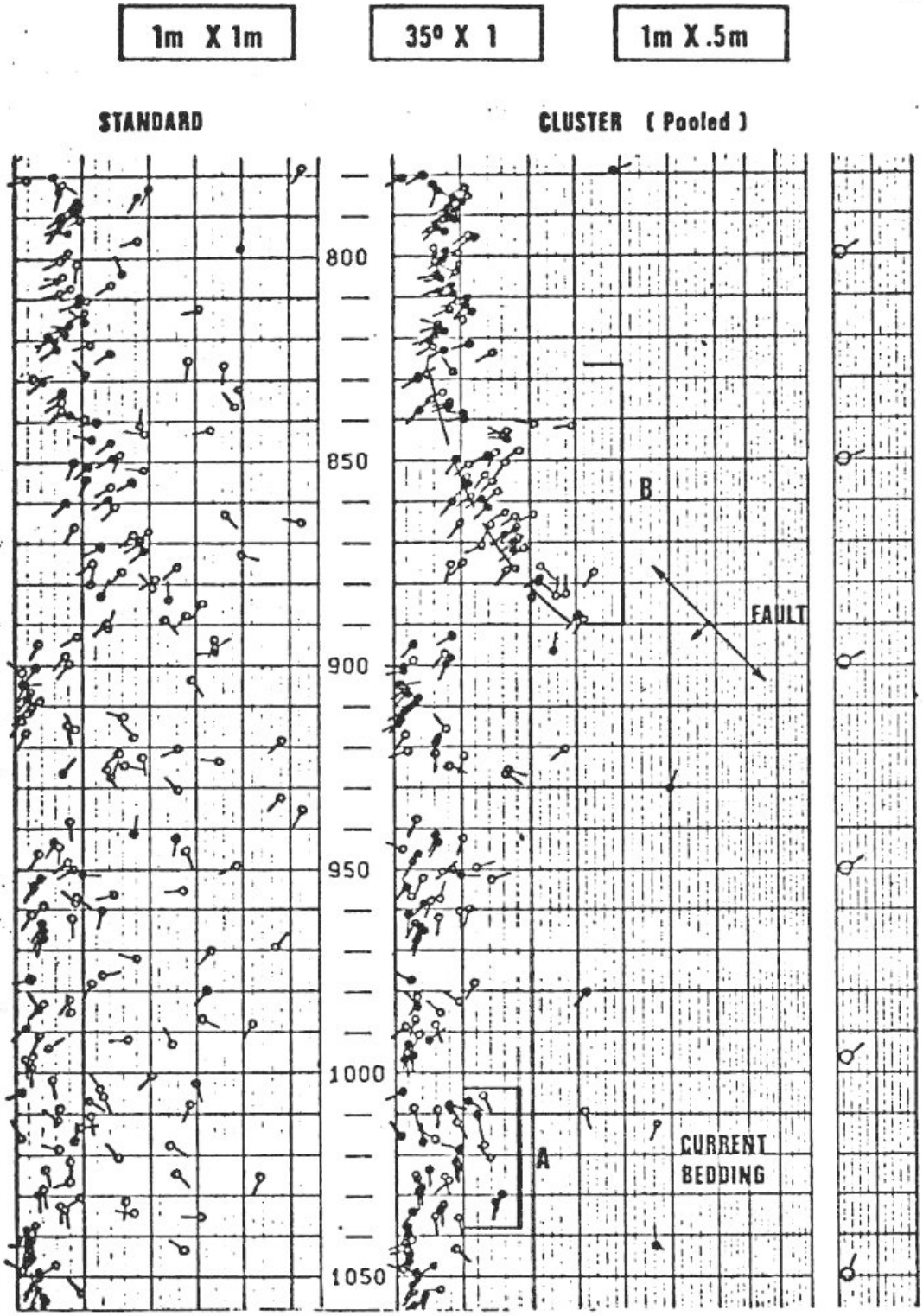

FIGURE 15 :

Results on the left have been obtained with the standard program. Results on the right were obtained with CLUSTER. The fault at 890 m is now clearly identified by a well defined "red" pattern (B) corresponding to drag on the down-thrown side. And cross-bedding exists in sand A which was not apparent with the standard processing.

APPLICATION OF THE HIGH RESOLUTION DIPMETER (HDT) * RESULTS TO REGIONAL WELL-TO-WELL CORRELATION

One of the concerns of the geologist is the determination of the dip of a formation. He is interested in the regional dip to help him map reservoirs, pin- point faults and unconformities, and generally solve structural problems. This was handled well enough by the 3 - arm dipmeter which in most cases gave satisfactory answers (10). But the last few years have seen a growing interest in more detailed stratigraphic analysis of reservoirs. Dips within a sedimentary unit or cycle give an indication as to direction and mode of deposition. And dips related to the boundaries of the units are supposedly indicative of the geometry of the reservoir. It becomes, through careful study of these dips, possible to estimate with reasonable accuracy the shape of a sand body. The strike, the lateral extent, the thickening and the location of the sediments' source can be derived from such a study for a given sand or group of sands (10) (11) (12). This type of analysis requires a maximum density of dips as the thickness of a depositional cycle can be quite small, down to the order of a few inches or less, and the density of occurences such as foreset beds within a cycle can be high. This strained the possibilities of the 3 - arm dipmeter to the point where a substitute had to be found if progress was to be made. The 4 - arm High Resolution Dipmeter (HDT) ensued.

The much improved vertical resolution of the HDT results in the curves being correlated having a high density of sharp correlatable features. Cases are known where as many as 10 correlations per foot are possible. Optical correlation then becomes too painstaking if one wants to make full use of the resolution. Therefore the data are recorded on a magnetic tape which is then fed to a computer. Through use of appropriate software, results are obtained at the requested density. I rge correlation intervals are used for structural applications while short correlation intervals, sometimes down to 1 foot or less, are used for detailed stratigraphic analysis. In order to eliminate random, accidental dips, the CLUSTER * program has been recently developed (13). One example is shown on Fig. 15. It allows taking full advantage of the resolution, while at the same time smoothing out the results for easier reading. Short of using very computer-time consuming and consequently expensive program doing with extreme accuracy what an optical correlator would do, this program is believed to obtain results as near as one can get to the true dips.

* Trade mark of Schlumberger.

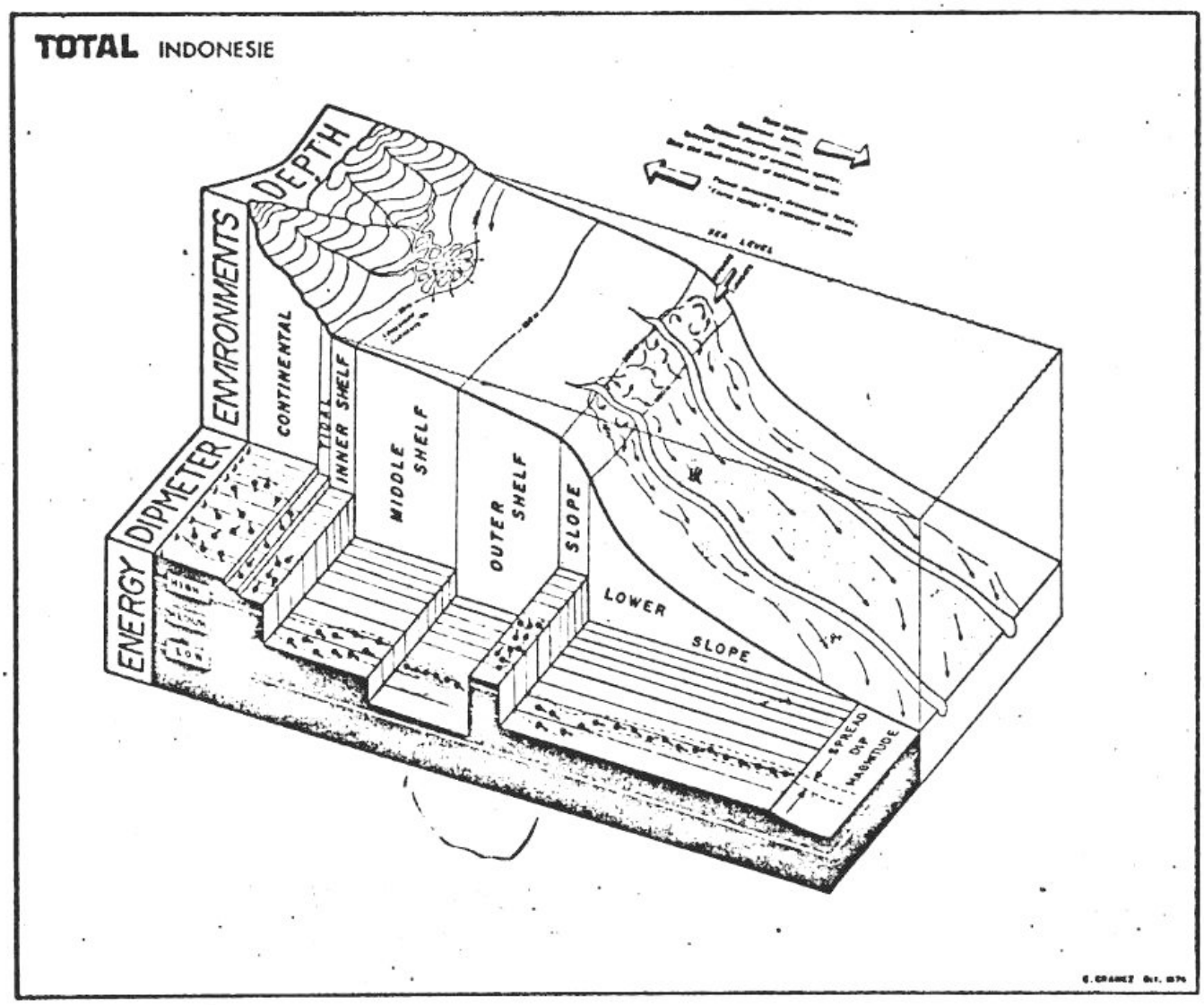

FIGURE 16 :

Relation between water depth, level of depositional energy and dipmeter results scatter

The high density of results obtained from the HDT has a side-effect which has proven to be very valuable. The early users were often puzzled by zone of great scatter in dip azimuth and magnitude. While some of these zones could be explained by mechanical reasons like hole damage while drilling, usually obvious on a caliper log, others did not fit this interpretation. It was thought early-on that the scatter was linked to the energy level prevailing during deposition (14) and three main energy levels were defined corresponding to:

- High energy - Continental, near shore (inner shelf)
- Medium energy - Delta fronts, Middle shelf
- Low energy - Outer shelf, abyssal deeps

The higher the energy, the larger the scatter of the dip magnitude.

Following this model, transgression and regression cycles can be recognized by studying the dip scatter. And it is possible to identify separate units within a sand which would otherwise have been considered as a whole (14).

As more HDT plots poured out, exceptions to that theory become evident. High energy zones identified from the scatter of results were proven by paleontological studies to have been deposited in deeper waters than predicted. So more thought was given to this apparent discrepancy and a logical explanation was found. The energy, low on the outer shelf, is high again where formations are deposited on the slope between outer shelf and abyssal deeps. The very fine grained marine shales slump while silts and looser sand grains slide down the slope to be deposited in deeper waters. So we can define a second cycle of 3 energy levels, resulting in the same appearance of the dipmeter results, from high on the upper slope to medium on the lower slope and low again in the abyssal deeps.

The environments associated with the 3 energy levels now become (15) (16) (Fig. 16):

1) High energy : 20° or more scatter of dip magnitude
   - Continental, near share (inner shelf)
   - Upper slope

2) Medium energy : 5° to 20° scatter
   - Delta fronts, middle shelf
   - Lower slope

3) Low energy : Less than 5° scatter
   - Outer shelf
   - Abyssal deeps, turbidites

As already mentioned, damage to the formation while drilling, caving and swelling shales can result in high dip spread which is not associated with depositional energy. A look at a caliper log is usually enough to identify and discard these zones as not representative.

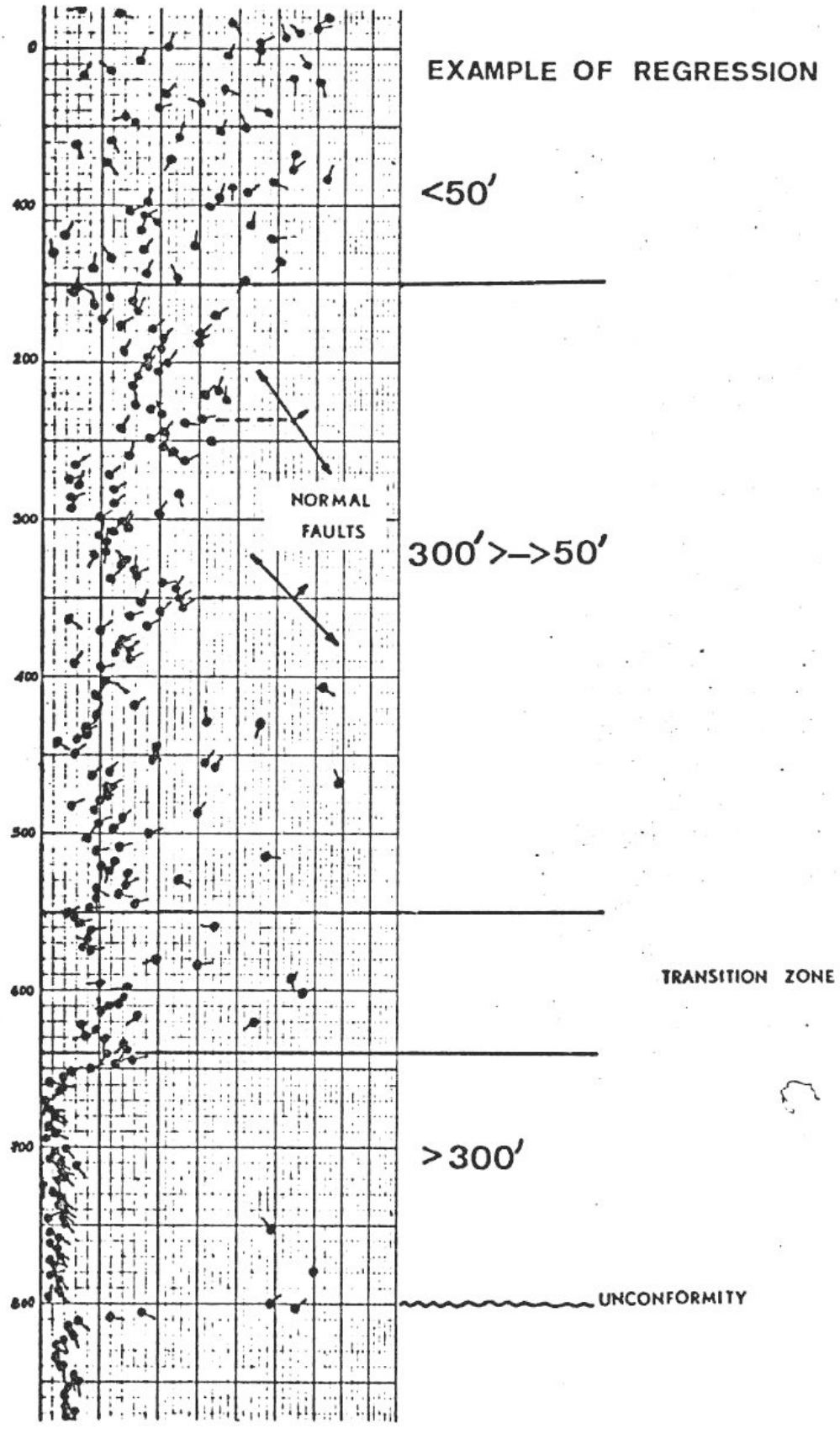

FIGURE 17 :

A continuous regressive phase from outer shelf below 650' to continental deposits above 150'. Water depths may vary from area to area for a given environment and must not be taken literally.

Another cause of scatter is faulting and / or weathering. The scatter here is due to reworking under high energy of sediments which may have been deposited with low energy. It is not related to depositional energy.

Fig. 17 shows a typical example of a complete regressive cycle from very low energy on the outer shelf to very high energy corresponding to continental deposits. An unconformity at 800' and faults at 350' and 235' result in dips being higher than expected from the environment. A few random high dips from 650' to 400' are due to hole damage (caving). It is otherwise a practically continuous sequence.

It is reasonable to assume that geological events of such amplitude corresponding to major shore line migrations occur on a basin wide scale and thus are correlatable over large distances. The next examples will illustrate this point.

Fig. 18 is an example of transgression followed by regression (16). Seven units can be identified :

a) High dips without significance in the basement.
b) High spread (30° - 40°) - High energy - Inner shelf from micropaleontology.
c) Low spread (4°) - Low energy - Micropaleontology indicates outer shelf. There is a short transition zone between b) and c) indicating that there was indeed transgression, probably rather rapid.
d) Medium to high spread (20° - 30°). Medium to high energy. Upper slope from micropaleontology.
e) Low spread (4° - 5°) - Could have been a continuation of the transgression and correspond to bathyal environment. In fact, micropaleontology indicates outer shelf. We have now entered the regressive phase. d) marked the end of the transgression.
f) High spread (30°) - High energy - Inner shelf
g) Very high spread (40°) - Very high energy - The absence of fauna and the lithology indicate a continental environment, marking the last stage of the regression.

The limit between transgression and regression is evident. There is an important break in dip dispersion (thus energy) from high to low, between upper slope and outer shelf. A slight difference in the position of this limit as given by HDT and by micropaleontology can be noted. This is no doubt due to scarcity of fauna and sampling interval.

This limit has been found in all the wells in the area and is considered as a time line. Based on this, regional well-to-well correlation becomes possible while it is difficult to impossible when using electric or nuclear (GR) logs only.

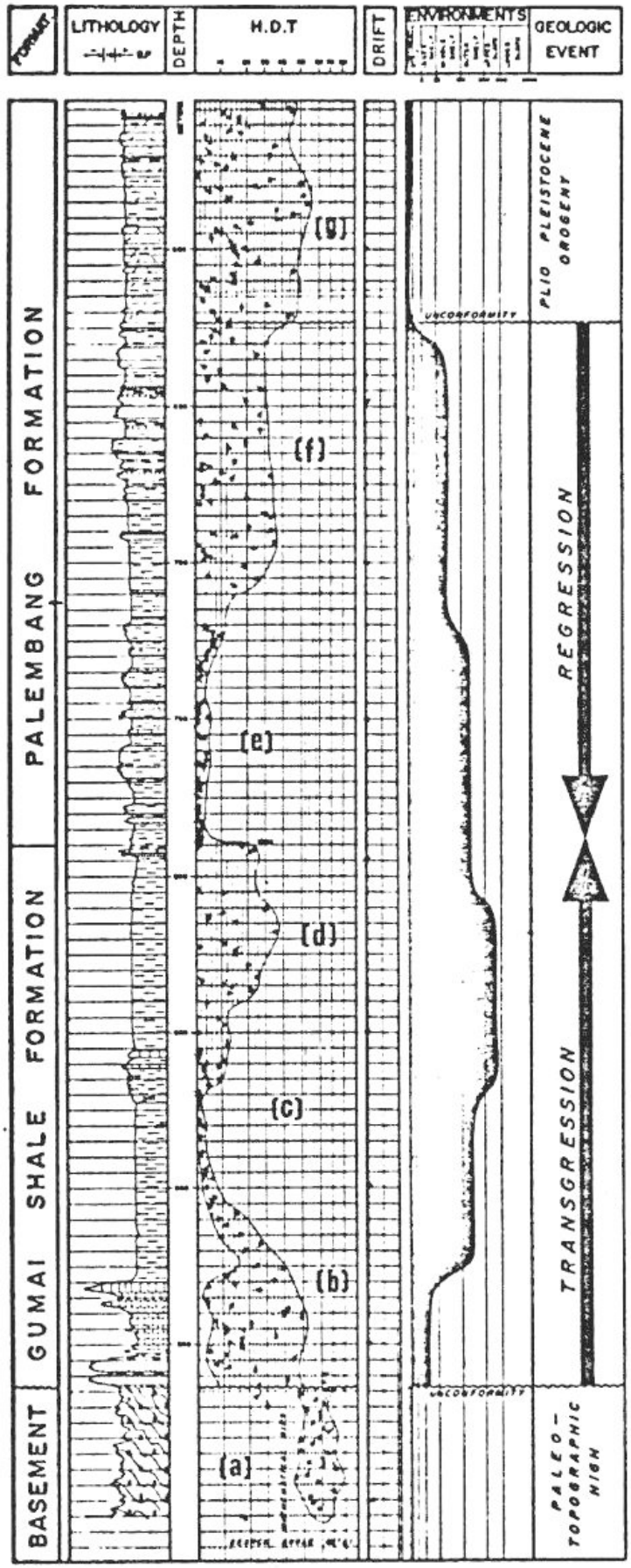

FIGURE 18 :

Transgression from inner shelf to outer slope characterizes the Gumai formation. It is followed immediately by regression to

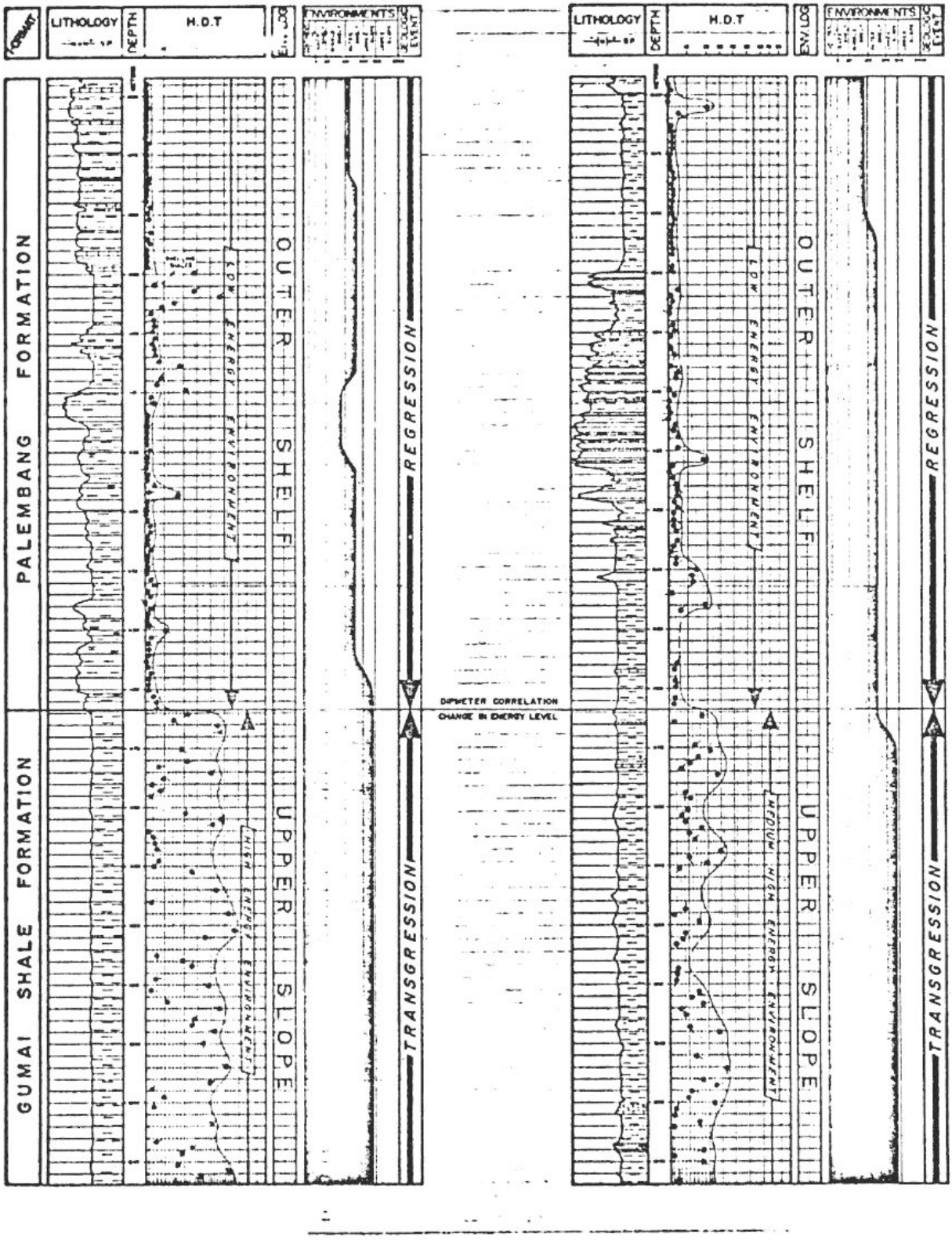

FIGURE 19 :

Correlation between two wells 10 kms apart. The limit between Gumai and Palembang is well defined by the dipmeters results as the apex of the transgression.

Fig. 19 shows an example of such a correlation between two wells about 10 kms apart. The start of the regressive sequence (Palembang Formation) is clearly defined on the dipmeter plot by a marked change in energy. Correlation from the logs usually ends the Gumai Formation at the first occurence of sands. Here conventional correlation would have started the Palembang on Well B at 1142 or 1136 m. Analysis of the dipmeter results puts it at 1162 m, or 20 m lower. Note also that the sands above 1090 m. in well A correspond to shales in well B. But the dipmeter results confirm that they have both been deposited with the same level of energy on the outer shelf as confirmed by paleontological data.

The High Resolution Dipmeter (HDT) is thus shown to be an " environment indicator" which can be used to recognize environments and to define broad units correlatable between wells far apart. As such, and in addition to its other uses like structural dip determination or reservoir geometry identification, it proves to be of great help to the exploration geologist when correlations based on conventional logs are difficult if not impossible because of lithology changes.

CONCLUSIONS

The new technologies presented here proved very valuable for both exploration and development purposes. A more accurate value of R_t (and consequently oil saturation) is obtained in many cases with the Dual-Laterolog (DLL) when the resistivity is high or the invasion pattern unfavourable for the induction log. Differentiation between gas and oil has been made easier by the combination Compensated Formation Density (FDC) - Dual-Spacing Neutron (CNL). The latter, little or not affected by the borehole, allows better porosity evaluation. And the CORIBAND program gives continuous accurate answers to the prime questions, oil saturation and porosity.

An additional but certainly not negligible feature of these new tools is their combinability. Two runs in the hole suffice to give the desired answers if the combinations DLL-MICROSFL and FDC-CNL are used. Their visual appeal is compounded by an appreciable gain in rig-time making them a must in development drilling.

The High Resolution Dipmeter has added a new dimension to the already considerable utility of the dipmeter results. Its good resolution has been enhanced by the use of the CLUSTER program. And its illustrated application to environment identification makes it a very valuable tool in exploration.

REFERENCES :

1) Schlumberger Log Interpretation Principles / Applications.

2) Schlumberger Log Interpretation Charts.

3) "Essentials of Log Interpretation Practice" - Schlumberger Document.

4) Souhaite, P., Misk, A. and Poupon, A. :
"R_t Determination in The Eastern Hemisphere".
SPWLA 16th Symposium, June 4 - 7, 1975.

5) Suan, J., Grimaldi, P., Poupon, A. and Souhaite, P. :
"The Dual Laterolog - R_{xo} Tool ".
SPE - AIME - 4018.

6) Alger, R.P., Locke, S., Nogel, W.A. and Sherman, H. :
"The Dual-Spacing Neutron Log - CNL".
JPT, September 1972.

7) Truman, R.B., Alger, R.P., Connel, J.G., Smith, R.L. :
"Progress Report on the Interpretation of the CNL in the U.S.".
SPWLA 13th Symposium, May 7 - 10, 1972.

8) Poupon, A. and Gaymard, R. :
"The Evaluation of Clay Content from Logs ".
SPWLA 11th Symposium, May 3 - 6, 1970.

9) Marchette, B. and Prins, W.J. :
"The Prediction of Water Cut in Initial Production from Log Analysis".
IPA 4th Convention, June 1976.

10) "Fundamentals of Dipmeter Interpretation" - Schlumberger Document.

11) Gilreath, J.A. and Maricelli, J.J. :
"Detailed Stratigraphic Control through Dip Computations".
A.A.P.G. Bulletin (December 1964) Volume 48, Number 12.

12) Campbell, R.L., Jr. :
"Stratigraphic Applications of Dipmeter in Mid-Continent".
A.A.P.G. Bulletin (September 1968) Volume 25, Number 9.

13) Hepp, V. and Dumestre, A.C. :
"CLUSTER. A Method for Selecting the Most Probable Dip Results from Dipmeter-Survey".
SPE 5543.

14) Gilreath, J.A., Healy, J.S. and Yelverton, J.N. :
"Depositional Environments Defined by Dipmeter Interpretation".

15) Gilreath, J.A. and Stephens, R.W. :
"Distributary Front Deposits Interpreted from Dipmeter Results".
Transactions GCAGS, 1971.

16) Cramez, C. :
"Stratigraphic Correlations and Sand Body Identification Using the HDT".
Internal report, Total Indonesie, May 1975.

17) Dadrian, C., Brown, H., Goetz, J. and Marchette, B. :
"Formation Evaluation in Indonesia".
SPWLA 14th Symposium, May 6 - 9, 1973.